# Efficient method to perform quantum number projection and configuration mixing for most general mean-field states

Shingo Tagami and Yoshifumi R. Shimizu

Department of Physics, Graduate School of Science,

Kyushu University, Fukuoka 812-8581, Japan

# Abstract

Combining several techniques, we propose an efficient and numerically reliable method to perform the quantum number projection and configuration mixing for most general mean-field states, i.e., the Hartree-Fock-Bogoliubov (HFB) type product states without symmetry restrictions. As for example of calculations, we show the results of the simultaneous parity, number and angular-momentum projection from HFB type states generated from the cranked Woods-Saxon mean-field with a very large basis that is composed of  $N_{\text{max}} = 20$  spherical harmonic oscillator shells.

#### I. INTRODUCTION

Recent advent of radioactive beam facilities is extending more and more widely the research area of nuclear physics. It is increasingly important to have a unified understanding of nuclear structure in various regions of the nuclear chart, with variety of ingredients such as shell effects, deformations and collective motions like rotation and vibration. Undoubtedly, the basic starting point is the selfconsistent mean-field approximation [1, 2], e.g., the Hartree-Fock (HF) or the Hartree-Fock-Bogoliubov (HFB) method including pairing correlations, with suitably chosen density-dependent effective interactions, or in a modern terminology, energy density functionals; see e.g. Ref. [3]. With the symmetry-breaking, relatively simple mean-field states can take into account most of the many-body correlations in a very efficient way [1, 2], and have been successfully applied to study various nuclear phenomena not only near the ground state but also in the low- to high-spin excited states [4–6].

However, the symmetry-breaking mean-field description is not enough because it represents merely the intrinsic state and the broken symmetry should be recovered in the laboratory frame. One of the most important consequences of the symmetry-breaking is the appearance of the symmetry-restoring collective motion. One well-adopted method to restore the symmetry is to utilize a phenomenological collective model like the rotor description in the unified model of Bohr-Mottelson [7]. One can consistently introduce the redundant collective coordinate into the many-body theory by employing the quantum mechanical constraint formalism (the gauge theory) between the nucleon and collective degrees of freedom, see e.g. Ref. [8]; its exact treatment is rather involved. Another way, without recourse to the external variables, to restore the symmetry within the nucleon degrees of freedom is the quantum number projection [1, 2]. Existence of a symmetrybreaking mean-field state means that all the states connected by the symmetry operation, e.g., rotation of the system, are degenerate. Superposition of all these degenerate states gives a better quantum mechanical description in the variational sense, as it is clear in the formulation of the generator coordinate method (GCM). Since the symmetry requires the specific form of weight functions for superposition, the procedure restores the symmetry at the same time, i.e., projects out the states with good quantum numbers.

The most important symmetry-breaking in nuclear structure is the spatial deformation,

e.g., the quadrupole shape, so that the projection of the angular momentum is necessary to obtain the eigenstates of the angular momentum operators, especially for calculating the electromagnetic transition probabilities. There is a long history in the angular momentum projection calculations. Except for some special calculations intended for very light nuclei, the general framework of the projection from the (HFB-like) general product-type meanfield wave functions has been developed by K. Hara and his collaborators in Refs. 9-11, where the calculation is restricted to the axially symmetric shape, but extended to the triaxially deformed and cranked (for high-spins) cases in Ref. [12] (see also the review paper [13], and a more recent application [14]). Based on the angular momentum projection, the variation after projection calculations from general mean-field states have also been performed for the G-matrix based realistic interactions, see e.g. Refs. [15, 16]. However, relatively small model spaces are used in these works, e.g., the two or three harmonic oscillator shells. Recently, the angular momentum projection with much larger space has been attempted with restriction of axially symmetry, intending to employ the Skyrme (or more general) energy functional [17], where the GCM calculation with respect to the quadrupole deformed coordinates on top of it is performed (see also Ref. [18] for the similar type calculation with the finite range Gogny interaction). The restriction of axial symmetry has been lifted in more recent works for the Skyrme [19], the relativistic meanfield [20, 21], and the Gogny [22] approaches, although still the time-reversal invariance (no-cranking) and the  $D_2$  symmetry of deformation are imposed in such calculations.

In this paper, we discuss an efficient method of general quantum number projection, i.e., rather technical aspect of projection. We intend to perform the angular momentum projection with other projections, the number and parity, at the same time from the most general symmetry-breaking HFB type mean-field, i.e., the axial symmetry, the parity, as well as the time-reversal invariance are broken. For this kind of the most general projection, the frequently used speed-up technique, for example, using the  $D_2$  symmetry that reduces the integration volume of the three Euler angles by factor 16, cannot be utilized. Therefore an efficient method to perform the projection is crucial. The basic ingredient of the projection is the overlap of operators between the product-type mean-field wave functions, based on the generalized Wick theorem [23, 24]. For evaluation of such overlaps many matrix operations composed of the multiplication, inverse and

determinant, are necessary, and so the dimension of matrices is the most crucial factor.

One of the essential ideas of our efficient method has been invented and discussed already in the Appendices of Ref. [25]; in fact we have noticed this reference after finishing our work (see also Refs. [17, 20, 26]). It is based on the fact that, although the model space for calculating the realistic single-particle states are large, the effective number of states contributing the HFB type product states are relatively small because the nuclear superfluidity is not so strong: If there is no pairing correlation, the mean-field state is a Slater determinant composed of the single-particle wave functions whose number is nothing else but the number of constituent particles. The truncation of the effective model space reduces the dimension of matrices dramatically in the most essential part of the calculation. Another important point of our method is that we make full use of the Thouless amplitudes rather than the (U, V) amplitudes of the generalized Bogoliubov transformation [1]. One of the reasons for this is that the sign of the norm overlap between general product-type wave functions can be precisely calculated by using their Thouless amplitudes [27]. Moreover, as a vacuum state, with respect to which the Thouless form of the general HFB type state is considered, we employ a suitably chosen Slater determinantal state, i.e., the particle-hole vacuum in place of the true nucleon vacuum is utilized. This increases the numerical stability of the Thouless amplitude  $(Z = (VU^{-1})^*)$  for the case of vanishing pairing correlations on one hand, and makes it possible to truncate further the space composed of deep hole states (the core contributions) on the other hand, which is very effective for calculations of heavy nuclei.

This article is organized as follows. The basic formulation of the efficient method to perform the general quantum number projection and/or the configuration mixing is presented in Sec. II. The results of example calculations are shown and discussed in Sec. III. Sec. IV is devoted to the summary.

#### II. FORMULATION

# A. Norm overlap, contractions, and generalized Wick theorem

Although the basic method of the projection (or GCM) is well-known [1, 9], we recapitulate it in order to fix the notation and explain our specific treatment (we mainly

follow the notation of Ref. [1]).

The Hamiltonian is composed of the one-body part and the two-body interaction,

$$\hat{H} = \sum_{l_1 l_2} t_{l_1 l_2} \hat{c}_{l_1}^{\dagger} \hat{c}_{l_2} + \frac{1}{2} \sum_{l_1 l_2 l_3 l_4} v_{l_1 l_2 l_3 l_4} \hat{c}_{l_1}^{\dagger} \hat{c}_{l_2}^{\dagger} \hat{c}_{l_4} \hat{c}_{l_3}, \tag{1}$$

whose explicit form is specified in the next section. Here  $(\hat{c}_l^{\dagger}, \hat{c}_l)$  (l=1,2,...,M) are the basic particle (nucleon) creation and annihilation operators, with M being the number of basis states. The appropriate choice of this original basis is very important to perform the angular momentum projection effectively. In this paper we choose the spherical (isotropic) harmonic oscillator basis,  $\{|Nljm\rangle\}$ , where the selection of the harmonic oscillator is optional; what is important is that the angular momentum (jm) is a good quantum number because the representation of the rotation matrix in this basis is block diagonal. Another possible choice for the case that the two-body interaction is local like the Skyrme and Gogny forces is the isotropic Cartesian harmonic oscillator basis, in which the rotation operator about one of the three axes is again represented by a block diagonal matrix with very few non-zero elements.

The fundamental object for the projection (or GCM) calculation is overlap  $\langle \Phi | \hat{O} | \Phi' \rangle$  of an arbitrary operator  $\hat{O}$  between two general product-type states  $|\Phi\rangle$  and  $|\Phi'\rangle$ . These mean-field states are vacuums of the quasiparticle operators,  $\hat{\beta}_k$  and  $\hat{\beta}'_k$ , respectively, which are related to the original particle basis by the following general Bogoliubov transformations,

$$\hat{\beta}_k^{\dagger} = \sum_{l} \left[ U_{lk} \hat{c}_l^{\dagger} + V_{lk} \hat{c}_l \right], \qquad \hat{\beta}_k^{\prime \dagger} = \sum_{l} \left[ U_{lk}^{\prime} \hat{c}_l^{\dagger} + V_{lk}^{\prime} \hat{c}_l \right]. \tag{2}$$

In most of realistic situations these (U, V) amplitudes are provided, although they contains redundant degree of unitary transformations between the quasiparticles for uniquely specifying the HFB type state [1]. In this subsection we assume that the states  $|\Phi\rangle$  and  $|\Phi'\rangle$  are not orthogonal to the true vacuum  $|\rangle$  of the original particle  $\hat{c}_l$ . Employing the Thouless theorem, these quasiparticle vacuums can be written explicitly as

$$|\Phi\rangle = n e^{\hat{Z}}|\rangle, \qquad \hat{Z} \equiv \frac{1}{2} \sum_{l'l} Z_{l'l} \hat{c}_{l'}^{\dagger} \hat{c}_{l}^{\dagger},$$

$$|\Phi'\rangle = n' e^{\hat{Z}'}|\rangle, \qquad \hat{Z}' \equiv \frac{1}{2} \sum_{l'l} Z'_{l'l} \hat{c}_{l'}^{\dagger} \hat{c}_{l}^{\dagger},$$
(3)

with normalization constants  $n \equiv \langle |\Phi\rangle$  and  $n' \equiv \langle |\Phi'\rangle$ , and the Thouless amplitudes Z

and Z' are defined in an obvious matrix notation by

$$Z \equiv (VU^{-1})^*, \qquad Z' \equiv (V'U'^{-1})^*. \tag{4}$$

In the following, we use the conventional matrix notations,  $A^{\dagger}$  (Hermitian conjugate),  $A^{T}$  (transpose),  $A^{*}$  (complex conjugate) and  $A^{-1}$  (matrix inverse), and further  $A^{-\dagger} \equiv (A^{\dagger})^{-1}$ ,  $A^{-T} \equiv (A^{T})^{-1}$  and  $A^{-*} \equiv (A^{*})^{-1}$ . Then, the norm overlap is given by

$$\langle \Phi | \Phi' \rangle = n^* n' \left( \det \left[ 1 + Z^{\dagger} Z' \right] \right)^{1/2} = n^* n' (-1)^{M(M+1)/2} \operatorname{pf} \begin{pmatrix} Z' & -1 \\ 1 & Z^{\dagger} \end{pmatrix},$$
 (5)

where the sign of square root of the determinant is uniquely fixed by the calculation of the pfaffian [27]. If we impose the normalization condition,  $\langle \Phi | \Phi \rangle = 1$  and  $\langle \Phi' | \Phi' \rangle = 1$ , the absolute value |n| and |n'| are determined. Using the identity  $|\det U|^2 = \det UU^{\dagger} = (\det [1 + Z^{\dagger}Z])^{-1}$ , we may write

$$n = e^{i\theta} (\det U^*)^{1/2}, \qquad n' = e^{i\theta'} (\det U'^*)^{1/2},$$
 (6)

where the quantities  $e^{i\theta}$  and  $e^{i\theta'}$  fix the phases of the states  $|\Phi\rangle$  and  $|\Phi'\rangle$ , respectively.

The overlap of an arbitrary operator is calculated according to the generalized Wick theorem [23, 24]; for example, for the two-body interaction,

$$\frac{\langle \Phi | \hat{c}_{l_1}^{\dagger} \hat{c}_{l_2}^{\dagger} \hat{c}_{l_4} \hat{c}_{l_3} | \Phi' \rangle}{\langle \Phi | \Phi' \rangle} = \rho_{l_3 l_1}^{(c)} \rho_{l_4 l_2}^{(c)} - \rho_{l_4 l_1}^{(c)} \rho_{l_3 l_2}^{(c)} + \bar{\kappa}_{l_2 l_1}^{(c)} \kappa_{l_3 l_4}^{(c)}, \tag{7}$$

where the basic contractions, or the transition density matrix  $\rho^{(c)}$  and the transition pairing tensors,  $\kappa^{(c)}$  and  $\bar{\kappa}^{(c)}$  with respect to the original particle basis  $(\hat{c}^{\dagger}, \hat{c})$  are defined by

$$\rho_{l'l}^{(c)} \equiv \frac{\langle \Phi | \hat{c}_{l}^{\dagger} \hat{c}_{l'} | \Phi' \rangle}{\langle \Phi | \Phi' \rangle} = \left( Z' \left[ 1 + Z^{\dagger} Z' \right]^{-1} Z^{\dagger} \right)_{l'l}, 
\kappa_{l'l}^{(c)} \equiv \frac{\langle \Phi | \hat{c}_{l} \hat{c}_{l'} | \Phi' \rangle}{\langle \Phi | \Phi' \rangle} = \left( Z' \left[ 1 + Z^{\dagger} Z' \right]^{-1} \right)_{l'l}, 
\bar{\kappa}_{l'l}^{(c)} \equiv \frac{\langle \Phi | \hat{c}_{l}^{\dagger} \hat{c}_{l'}^{\dagger} | \Phi' \rangle}{\langle \Phi | \Phi' \rangle} = \left( \left[ 1 + Z^{\dagger} Z' \right]^{-1} Z^{\dagger} \right)_{l'l}.$$
(8)

In Ref. [9], for example, the contractions between the quasiparticles  $\hat{\beta}_k$  and  $\hat{\beta}'_k$  are given in terms of the coefficients of generalized Bogoliubov transformation between them. However, it is shown in the following subsections that the truncation of the effective model space can be done in a more transparent manner if the Thouless amplitudes are utilized.

## B. Quantum number projection

A state with good quantum numbers is obtained by the projection from the symmetry-breaking mean-field state  $|\Phi\rangle$  [1],

$$|\alpha\rangle = \hat{P}_{\alpha}|\Phi\rangle, \qquad \hat{P}_{\alpha} = \int g_{\alpha}(\boldsymbol{x})\hat{D}(\boldsymbol{x})d\boldsymbol{x}.$$
 (9)

Here  $\alpha$  denotes a set of quantum numbers, and the projection operator  $\hat{P}_{\alpha}$  is defined by the superposition of all possible unitary transformations  $\hat{D}(\boldsymbol{x})$  with the weight function  $g_{\alpha}(\boldsymbol{x})$ , where the continuous parameters  $\boldsymbol{x} \equiv (x_1, x_2, ...)$  specify the coordinates in the manifold of symmetry operations. In the case of the number and the angular momentum projection, it is written as  $\hat{D}(\boldsymbol{x}) = e^{i\varphi\hat{N}}\hat{R}(\omega)$  with the gauge angle  $\varphi$  and the Euler angles  $\omega$  as parameters  $\boldsymbol{x}$ , where  $\hat{N}$  is the number operator and  $\hat{R}(\omega)$  is the rotation operator. Note that the parity projector,

$$\hat{P}_{\pm} = \frac{1}{2} \left[ 1 \pm \hat{\Pi} \right],\tag{10}$$

where  $\hat{\Pi}$  is the space inversion operator, has the same form as in Eq. (9), although the values of parameter are discrete.

General quantum-number-projection calculation requires to evaluate the matrix elements,  $\langle \Phi | \hat{P}_{\alpha} \hat{O} \hat{P}_{\alpha'} | \Phi' \rangle$ , between two general product-type states  $|\Phi\rangle$  and  $|\Phi'\rangle$  for arbitrary operator  $\hat{O}$ . Since the operator  $\hat{O}$ , e.g., the Hamiltonian or the electromagnetic transition operators, usually belongs to an irreducible representation of the symmetry transformation  $\hat{D}(\boldsymbol{x})$  associated with the projector, it is enough to consider either  $\langle \Phi | \hat{O} \hat{D}(\boldsymbol{x}) | \Phi' \rangle$  or  $\langle \Phi | \hat{D}(\boldsymbol{x}) \hat{O} | \Phi' \rangle$  at mesh points of numerical integration over the parameter space  $(\boldsymbol{x})$ . We employ the form where the unitary transformation is on the right in the following, but one can use another form with trivial modifications.

In the following we omit to denote the parameters  $\boldsymbol{x}$  in the unitary transformation  $\hat{D}$  as long as there is no confusion. In the usual projection calculations, the unitary transformation is generated by a one-body Hermitian operator  $\hat{G}$  ( $\hat{G}^{\dagger} = \hat{G}$ ); most generally,

$$\hat{D} = e^{i\hat{G}}, \qquad \hat{G} = g^0 + \sum_{ll'} g_{ll'}^{11} \hat{c}_l^{\dagger} \hat{c}_{l'} + \frac{1}{2} \sum_{ll'} \left( g_{ll'}^{20} \hat{c}_l^{\dagger} \hat{c}_{l'}^{\dagger} + \text{h.c.} \right). \tag{11}$$

The norm overlap of two normalized HFB type states  $|\Phi\rangle$  and  $|\Phi'\rangle$  in the Thouless form is given in Eq. (5) with the normalization constants in Eq. (6). If the one state is the

unitary transformed state of the other,  $|\Phi'\rangle = \hat{D}|\Phi\rangle$ , the relative phase between them is determined uniquely [9]. Namely, the difference between  $\theta'$  and  $\theta$  in Eq. (6) in such a case is given by

$$\theta' - \theta = g^0 + \frac{1}{2} \operatorname{Tr} g^{11} \equiv \Theta(\hat{D}), \tag{12}$$

and then the norm overlap can be calculated as

$$\langle \Phi | \hat{D} | \Phi \rangle = e^{i\Theta(\hat{D})} \left( \det \mathcal{U}^* \right)^{1/2}, \qquad \mathcal{U} = U^{\dagger} U' + V^{\dagger} V'.$$
 (13)

### C. Model space truncation

The occupation probabilities of the original particle basis are not necessarily small for a given quasiparticle vacuum state  $|\Phi\rangle$ ,

$$\langle \Phi | \hat{c}_l^{\dagger} \hat{c}_l | \Phi \rangle \neq 0, \quad l = 1, 2, ..., M.$$
 (14)

However, the superfluidity of nuclei is not so strong in most cases and the effective number of basis states contributing to the state  $|\Phi\rangle$  is relatively small: It can be clearly recognized by introducing a canonical-like basis that diagonalizes the usual density matrix  $\rho_{l'l} \equiv \langle \Phi | \hat{c}_l^{\dagger} \hat{c}_{l'} | \Phi \rangle / \langle \Phi | \Phi \rangle$ ;

$$\hat{b}_k^{\dagger} = \sum_l W_{lk} \hat{c}_l^{\dagger}, \quad WW^{\dagger} = W^{\dagger}W = 1, \tag{15}$$

$$\rho = W \bar{\rho} W^{\dagger}, \quad \bar{\rho} = \text{diag}(v_1^2, v_2^2, ...),$$
(16)

where the occupation probabilities  $v_k^2 = \langle \Phi | \hat{b}_k^{\dagger} \hat{b}_k | \Phi \rangle$  (k = 1, 2, ..., M), which are at least pairwisely degenerate, are assumed to be in descending order (i.e.,  $v_1^2 = v_2^2 \ge v_3^2 = v_4^2 \ge$  ...). Then most of  $v_k$ 's are negligibly small; more precisely, we take some small number  $\epsilon$  and select the P space composed of  $L_p(\epsilon)$  orbits which satisfy  $v_k^2 \ge \epsilon$   $(k = 1, 2, ..., L_p(\epsilon))$ , while in the complemental Q (= 1 - P) space we set  $v_k = 0$   $(k = L_p(\epsilon) + 1, ..., M)$ . Practically the parameter  $\epsilon$  is chosen to be as large as possible within the condition that the final results (e.g., the energy spectra) do not change; we find that typically  $\epsilon = 10^{-4} - 10^{-5}$  is enough. For example, if we use a Woods-Saxon potential, the typical number of spherical oscillator shells necessary is  $N_{\rm osc} \approx 12 - 14$  for heavy stable nuclei. However, it can happen that one should include more shells, e.g., up to  $N_{\rm osc} \approx 20$ , to describe weakly bound orbits correctly, then M > 3000. It turns out that the effective

number of the P space stays  $L_p(\epsilon) \approx 100 - 250$  in most of the cases (for either neutrons or protons), which are about one order of magnitude smaller than the number of original basis states M. In Ref. [29], this fact is used and a very efficient method is developed to solve the HFB equation in terms of the small number of canonical basis (note that the canonical basis is usually calculated after obtaining the HFB state).

Employing the Block-Messiah theorem, the amplitudes of the Bogoliubov transformation in Eq. (2) is written as

$$U = W\bar{U}C, \quad V = W^*\bar{V}C, \tag{17}$$

where the matrices W (the one in Eq. (15)) and C are unitary, and  $(\bar{U}, \bar{V})$  are of the so-called canonical form [1] if the basis is rigorously canonical, which is not necessarily required in the following discussion. According to the P and Q space decomposition defined above, they are in the following block forms,

$$W = \begin{pmatrix} W_p & W_q \end{pmatrix}, \quad \bar{U} = \begin{pmatrix} \bar{U}_{pp} & 0 \\ 0 & 1 \end{pmatrix}, \quad \bar{V} = \begin{pmatrix} \bar{V}_{pp} & 0 \\ 0 & 0 \end{pmatrix}. \tag{18}$$

where obviously, for example,  $W_p$  is  $M \times L_p$  matrix and  $\bar{U}_{pp}$  is  $L_p \times L_p$  matrix (dropping  $\epsilon$  for simplicity). Although the effective number of the P space  $(L_p)$  is relatively small, it should be noted that calculations of the projection, especially the angular momentum projection, are not confined within this space. This is because of the symmetry-breaking feature of the general quasiparticle state  $|\Phi\rangle$ ; the transformation in the projection operation (e.g. the rotation) kicks the orbits belonging to the P space out of the model space.

For the number or angular momentum projection, the one-body generator  $\hat{G}$  of the symmetry transformation  $\hat{D}$  in Eq. (11) has no  $g^{20}$  terms in the original basis;

$$\hat{G} = g^0 + \sum_{ll'} g_{ll'}^{11} \hat{c}_l^{\dagger} \hat{c}_{l'}, \tag{19}$$

and then the  $M \times M$  transformation matrix D in the original basis  $\hat{c}_l$  is defined by

$$\hat{D}\hat{c}_{l}^{\dagger}\hat{D}^{\dagger} = \sum_{l'} D_{l'l}\hat{c}_{l'}^{\dagger}, \qquad D = \exp(ig^{11}). \tag{20}$$

Then, assuming the normalization,  $\langle \Phi | \Phi \rangle = 1$ , and using the identity  $\exp(i \operatorname{Tr} g^{11}) = \det D$ , the norm overlap in Eq. (13) is explicitly written as

$$\langle \Phi | \hat{D} | \Phi \rangle = e^{ig^0} \left( \det D \det \mathcal{U}^* \right)^{1/2} = e^{ig^0} \left( \det \tilde{D} \det \bar{\mathcal{U}}^* \right)^{1/2}, \tag{21}$$

with

$$\mathcal{U} = U^{\dagger}DU + V^{\dagger}D^*V = C^{\dagger}\bar{\mathcal{U}}C, \qquad \bar{\mathcal{U}} = \bar{U}^{\dagger}\tilde{D}\bar{U} + \bar{V}^{\dagger}\tilde{D}^*\bar{V}. \tag{22}$$

The matrix  $\tilde{D}$  is the transformation matrix in the canonical basis  $(\hat{b}^{\dagger}, \hat{b})$ ,

$$\tilde{D} \equiv W^{\dagger}DW = \begin{pmatrix} W_p^{\dagger}DW_p & W_p^{\dagger}DW_q \\ W_q^{\dagger}DW_p & W_q^{\dagger}DW_q \end{pmatrix} \equiv \begin{pmatrix} \tilde{D}_{pp} & \tilde{D}_{pq} \\ \tilde{D}_{qp} & \tilde{D}_{qq} \end{pmatrix}, \tag{23}$$

with which the matrix  $\bar{\mathcal{U}}$  is of the form,

$$\bar{\mathcal{U}} = \begin{pmatrix} \bar{U}_{pp}^{\dagger} \tilde{D}_{pp} \bar{U}_{pp} + \bar{V}_{pp}^{\dagger} \tilde{D}_{pp}^{*} \bar{V}_{pp} & \bar{U}_{pp}^{\dagger} \tilde{D}_{pq} \\ \tilde{D}_{qp} \bar{U}_{pp} & \tilde{D}_{qq} \end{pmatrix} \equiv \begin{pmatrix} \bar{\mathcal{U}}_{pp} & \bar{\mathcal{U}}_{pq} \\ \bar{\mathcal{U}}_{qp} & \bar{\mathcal{U}}_{qq} \end{pmatrix}. \tag{24}$$

Since there are no reasons to expect that the transformation matrix related to the Q space,  $\tilde{D}_{qp}$  or  $\tilde{D}_{qq}$ , is small in any sense, the number of dimension to calculate the determinant of the norm overlap in Eq. (21) cannot be reduced. However, as it is mentioned in the Appendices in Refs. [20, 25], the model space truncation in terms of (U, V) amplitudes is possible, which can be naturally derived by the following treatment in terms of the Thouless amplitude: We demonstrate it in the Appendix.

On the other hand, if we change the notation and consider the Thouless form of the state  $|\Phi\rangle$  with respect to the canonical basis  $\hat{b}_k$ ,

$$|\Phi\rangle = n e^{\hat{Z}}|\rangle, \quad \hat{Z} \equiv \frac{1}{2} \sum_{k'k} Z_{k'k} \hat{b}_{k'}^{\dagger} b_{k}^{\dagger},$$
 (25)

with the definition,

$$Z \equiv (\bar{V}\bar{U}^{-1})^* = \begin{pmatrix} (\bar{V}_{pp}\bar{U}_{pp}^{-1})^* & 0\\ 0 & 0 \end{pmatrix} = \begin{pmatrix} Z_{pp} & 0\\ 0 & 0 \end{pmatrix}, \tag{26}$$

the norm overlap (21) can be easily calculated (see the next subsection for details) as

$$\langle \Phi | \hat{D} | \Phi \rangle = e^{ig^0} | \det \bar{U} | \left( \det \left[ 1 + Z^{\dagger} Z_D \right] \right)^{1/2}, \tag{27}$$

where the transformed Thouless amplitude  $Z_D$  is introduced by

$$Z_D \equiv \tilde{D}Z\tilde{D}^T = \begin{pmatrix} \tilde{D}_{pp}Z_{pp}\tilde{D}_{pp}^T & \tilde{D}_{pp}Z_{pp}\tilde{D}_{qp}^T \\ \tilde{D}_{qp}Z_{pp}\tilde{D}_{pp}^T & \tilde{D}_{qp}Z_{pp}\tilde{D}_{qp}^T \end{pmatrix}.$$
(28)

The non-trivial point for the model space truncation is that the amplitude  $Z_D$  is not confined within the P space in contrast to Z. However, the matrix appearing in the norm overlap is of the form,

$$1 + Z^{\dagger} Z_{D} = \begin{pmatrix} 1 + Z_{pp}^{\dagger} Z_{Dpp} & Z_{pp}^{\dagger} Z_{Dpq} \\ 0 & 1 \end{pmatrix}, \tag{29}$$

so that the determinant in Eq. (27) can be calculated within the P space only,

$$\det\left[1 + Z^{\dagger}Z_{D}\right] = \det\left[1 + Z_{pp}^{\dagger}Z_{Dpp}\right],\tag{30}$$

where we simply use the notation like  $Z_{pp}^{\dagger} \equiv (Z_{pp})^{\dagger}$  if there is no confusion. Namely, the dimension of the determinant is reduced from M to  $L_p$ , if one uses the representation in terms of the Thouless amplitude. In the next subsection we show that not only the norm overlap but also most part of calculations of the contractions can be done within the truncated P space for general cases, and the amount of calculation is greatly reduced by employing the Thouless amplitudes.

## D. Calculation within truncated space

As is discussed in the previous subsections, the quantity to be calculated is  $\langle \Phi | \hat{O} \hat{D} | \Phi' \rangle$  for an arbitrary operator  $\hat{O}$  with the unitary transformation  $\hat{D}$  of the symmetry operation. Using the generalized Wick theorem, its evaluation reduces to calculate the following basic contractions (or overlaps),

$$\begin{pmatrix} \rho_D^{(c)} \rangle_{l'l} \equiv \langle \Phi | \hat{c}_l^{\dagger} \hat{c}_{l'} [\hat{D}] | \Phi' \rangle, \\
\begin{pmatrix} \kappa_D^{(c)} \rangle_{l'l} \equiv \langle \Phi | \hat{c}_l \hat{c}_{l'} [\hat{D}] | \Phi' \rangle, \\
\begin{pmatrix} \bar{\kappa}_D^{(c)} \rangle_{l'l} \equiv \langle \Phi | \hat{c}_l^{\dagger} \hat{c}_{l'} [\hat{D}] | \Phi' \rangle, \end{pmatrix} \tag{31}$$

with the definition

$$[\hat{D}] \equiv \hat{D}/\langle \Phi | \hat{D} | \Phi' \rangle,$$
 (32)

where the argument (x) is simply omitted. In this subsection we develop the efficient method to evaluate the contractions above as well as the norm overlap  $\langle \Phi | \hat{D} | \Phi' \rangle$  applying the truncation scheme explained in the previous subsection.

Thus, we introduce two bases associated with two HFB type states  $|\Phi\rangle$  and  $|\Phi'\rangle$ ,

$$\hat{b}_k^{\dagger} = \sum_{l} W_{lk} \hat{c}_l^{\dagger}, \qquad \hat{b}_k'^{\dagger} = \sum_{l} W_{lk}' \hat{c}_l^{\dagger}, \tag{33}$$

respectively, with the transformation matrices  $W = (W_p, W_q)$  and  $W' = (W'_{p'}, W'_{q'})$ , where the two bases satisfy

$$\hat{b}_k |\Phi\rangle = 0, \quad k > L_p, \qquad \hat{b}'_{k'} |\Phi'\rangle = 0, \quad k' > L_{p'}, \tag{34}$$

namely, the submatrices  $W_p$  and  $W'_{p'}$  are  $M \times L_p$  and  $M \times L_{p'}$ , respectively. The quantity  $L_p(L_{p'})$  defines the dimension of the P space for  $|\Phi\rangle$  ( $|\Phi'\rangle$ ). These bases operators ( $\hat{b}^{\dagger}, \hat{b}$ ) and ( $\hat{b}'^{\dagger}, \hat{b}'$ ) are practically obtained by diagonalizing the density matrices for  $|\Phi\rangle$  and  $|\Phi'\rangle$  like in Eq. (16), but one should note that they are not necessarily the canonical bases if there exist extra degeneracies for the occupation numbers. Therefore we call them canonical-like bases. We introduce the Thouless amplitudes for these bases ( $\hat{b}^{\dagger}, \hat{b}$ ) and ( $\hat{b}'^{\dagger}, \hat{b}'$ ) as

$$|\Phi\rangle = n e^{\hat{Z}}|\rangle, \qquad \hat{Z} \equiv \sum_{k' < k} Z_{k'k} \hat{b}_{k'}^{\dagger} \hat{b}_{k}^{\dagger}, \qquad Z = -Z^{T},$$

$$|\Phi'\rangle = n' e^{\hat{Z}'}|\rangle, \qquad \hat{Z}' \equiv \sum_{k' < k} Z'_{k'k} \hat{b}'_{k'}^{\dagger} \hat{b}'_{k}^{\dagger}, \qquad Z' = -Z'^{T}.$$

$$(35)$$

Here n and n' are normalization constants of the vacuum states  $|\Phi\rangle$  and  $|\Phi'\rangle$ , which are not specified here. Note that the Thouless amplitudes Z(Z') defined by Eq. (35) can be calculated from the original (U, V) ((U', V')) amplitudes and W(W') for given state  $|\Phi\rangle$   $(|\Phi'\rangle)$ , and is essentially  $L_p \times L_p$   $(L_{p'} \times L_{p'})$  matrix, i.e.

$$Z = W^{\dagger}(VU^{-1})^*W^* = \begin{pmatrix} Z_{pp} & 0 \\ 0 & 0 \end{pmatrix}, \quad Z' = W'^{\dagger}(V'U'^{-1})^*W'^* = \begin{pmatrix} Z'_{p'p'} & 0 \\ 0 & 0 \end{pmatrix}$$
(36)

The unitary transformation  $\hat{D}$  in Eq. (19) induces the transformation between the two bases  $(\hat{b}^{\dagger}, \hat{b})$  and  $(\hat{b}'^{\dagger}, \hat{b}')$ ,

$$\hat{D}\hat{b}_{k}^{'\dagger}\hat{D}^{\dagger} = \sum_{k'} \tilde{D}_{k'k}\hat{b}_{k}^{\dagger}, \quad \hat{D}^{\dagger}\hat{b}_{k}^{\dagger}\hat{D} = \sum_{k'} \tilde{D}_{kk'}^{*}\hat{b}_{k'}^{\dagger}, \tag{37}$$

with the definition similarly to Eq. (23),

$$\tilde{D} \equiv W^{\dagger}DW' = \begin{pmatrix} W_p^{\dagger}DW'_{p'} & W_p^{\dagger}DW'_{q'} \\ W_q^{\dagger}DW'_{p'} & W_q^{\dagger}DW'_{q'} \end{pmatrix} \equiv \begin{pmatrix} \tilde{D}_{pp'} & \tilde{D}_{pq'} \\ \tilde{D}_{qp'} & \tilde{D}_{qq'} \end{pmatrix}, \tag{38}$$

where the transformation matrix D in the original basis  $(\hat{c}^{\dagger}, \hat{c})$  is defined in Eq. (20), and the induced matrix  $\tilde{D}_{pp'}$  in the P space, for example, is now rectangular and a  $L_p \times L_{p'}$ matrix. The action of  $\hat{D}$  on the quasi-particle vacuum  $|\Phi'\rangle$  can be calculated as

$$\hat{D}|\Phi'\rangle = n' \exp(\hat{D}\hat{Z}'\hat{D}^{\dagger})\hat{D}|\rangle = n' e^{\hat{Z}'_D}|\rangle e^{ig_0}, \tag{39}$$

with

$$\hat{Z}_D' \equiv \hat{D}\hat{Z}'\hat{D}^{\dagger} = \sum_{l' < l} Z_{Dl'l}'\hat{b}_{l'}^{\dagger}\hat{b}_{l}^{\dagger}, \tag{40}$$

where the transformed Thouless amplitude similar to Eq. (28) is defined by

$$Z'_{D} \equiv \tilde{D}Z'\tilde{D}^{T} = \begin{pmatrix} \tilde{D}_{pp'}Z'_{p'p'}\tilde{D}^{T}_{pp'} & \tilde{D}_{pp'}Z'_{p'p'}\tilde{D}^{T}_{qp'} \\ \tilde{D}_{qp'}Z'_{p'p'}\tilde{D}^{T}_{pp'} & \tilde{D}_{qp'}Z'_{p'p'}\tilde{D}^{T}_{qp'} \end{pmatrix} \equiv \begin{pmatrix} Z'_{Dpp} & Z'_{Dpq} \\ Z'_{Dqp} & Z'_{Dqq} \end{pmatrix}, \tag{41}$$

which is not confined in the P space. Then similarly to Eq.(30) the norm overlap can be evaluated within the P space as

$$\langle \Phi | \hat{D} | \Phi' \rangle = n^* n' e^{ig_0} \left( \det \left[ 1 + Z_{pp}^{\dagger} Z_{Dpp}' \right] \right)^{1/2}$$

$$= n^* n' \langle |\hat{D}| \rangle (-1)^{L_p(L_p+1)/2} \operatorname{pf} \begin{pmatrix} Z_{Dpp}' & -1 \\ 1 & Z_{pp}^{\dagger} \end{pmatrix}. \tag{42}$$

Namely the dimension of matrix is reduced from M to  $L_p$ .

The basic contractions can be calculated through the canonical-like basis  $(\hat{b}^{\dagger}, \hat{b})$ ,

$$\rho_D^{(c)} = W \rho_D^{(b)} W^{\dagger}, \qquad \kappa_D^{(c)} = W \kappa_D^{(b)} W^T, \qquad \bar{\kappa}_D^{(c)} = W^* \bar{\kappa}_D^{(b)} W^{\dagger}, \tag{43}$$

where

$$\begin{pmatrix} \rho_D^{(b)} \end{pmatrix}_{k'k} \equiv \langle \Phi | \hat{b}_k^{\dagger} \hat{b}_{k'} [\hat{D}] | \Phi' \rangle = \left( Z_D' \left[ 1 + Z^{\dagger} Z_D' \right]^{-1} Z^{\dagger} \right)_{k'k}, 
\left( \kappa_D^{(b)} \right)_{k'k} \equiv \langle \Phi | \hat{b}_k \hat{b}_{k'} [\hat{D}] | \Phi' \rangle = \left( Z_D' \left[ 1 + Z^{\dagger} Z_D' \right]^{-1} \right)_{k'k}, 
\left( \bar{\kappa}_D^{(b)} \right)_{k'k} \equiv \langle \Phi | \hat{b}_k^{\dagger} \hat{b}_{k'}^{\dagger} [\hat{D}] | \Phi' \rangle = \left( \left[ 1 + Z^{\dagger} Z_D' \right]^{-1} Z^{\dagger} \right)_{k'k}.$$
(44)

Using the corresponding equation to (29),

$$\bar{\kappa}_{D}^{(b)} = \begin{pmatrix} [1 + Z_{pp}^{\dagger} Z_{Dpp}]^{-1} Z_{pp}^{\dagger} & 0 \\ 0 & 0 \end{pmatrix} \equiv \begin{pmatrix} \bar{\kappa}_{Dpp}^{(b)} & 0 \\ 0 & 0 \end{pmatrix}, \tag{45}$$

which has only the P space components. Further using the identities

$$\rho^{(b)} = Z_D' \bar{\kappa}_D^{(b)}, \qquad \kappa_D^{(b)} = Z_D' - \rho_D^{(b)} Z_D' = Z_D' - Z_D' \bar{\kappa}_D^{(b)} Z_D', \tag{46}$$

which can be easily confirmed by Eq. (44), we have

$$\rho_{D}^{(c)} = DW'_{p'} (Z'_{p'p'} \tilde{D}^{T}_{pp'} \bar{\kappa}^{(b)}_{Dpp}) W_{p}^{\dagger}, 
\kappa_{D}^{(c)} = DW'_{p'} (Z'_{p'p'} - Z'_{p'p'} \tilde{D}^{T}_{pp'} \bar{\kappa}^{(b)}_{Dpp} \tilde{D}_{pp'} Z'_{p'p'}) W'^{T}_{p'} D^{T}, 
\bar{\kappa}_{D}^{(c)} = W_{p}^{*} (\bar{\kappa}^{(b)}_{Dpp}) W_{p}^{\dagger}.$$
(47)

Namely, most of the calculations, i.e., the part in parentheses in Eq. (47), can be done within the P space.

In order to make reduced calculations within the P space more systematically and to enable a generalization, which is discussed in the next subsection, we use the following property of the basis truncation defined in Eq. (34);

$$\hat{b}_{k}\hat{D}|\Phi'\rangle = \hat{D}\sum_{k'}\tilde{D}_{kk'}\hat{b}'_{k'}|\Phi'\rangle = \sum_{k_{n'}=1}^{L_{p'}}(\tilde{\tau}_{Dp'})_{kk_{p'}}\hat{b}_{k_{p'}}\hat{D}|\Phi'\rangle, \tag{48}$$

where a new  $M \times L_{p'}$  matrix  $\tilde{\tau}_{Dp'}$  is defined by

$$(\tilde{\tau}_{Dp'})_{kk_{p'}} \equiv \sum_{k'_{p'}=1}^{L_{p'}} \tilde{D}_{kk'_{p'}} \left(\tilde{D}_{P'}^{-1}\right)_{k'_{p'}k_{p'}}, \quad \text{i.e.,} \quad \tilde{\tau}_{Dp'} = W^{\dagger}DW'_{p'}\tilde{D}_{P'}^{-1}. \tag{49}$$

Here we have introduced an auxiliary  $L_{p'} \times L_{p'}$  square submatrix  $\tilde{D}_{P'}$  of  $\tilde{D}$ , and its inverse  $\tilde{D}_{P'}^{-1}$ , i.e.,

$$\tilde{D}_{P'} = (\tilde{D}_{kk'}; k, k' = 1, 2, ..., L_{p'}),$$
(50)

which should not be confused with the  $L_p \times L_{p'}$  submatrix  $\tilde{D}_{pp'}$  in Eq. (38) (of course,  $\tilde{D}_{pp'}$  and  $\tilde{D}_{P'}$  coincide if  $L_p = L_{p'}$ ). The P space should be chosen in such a way that the matrix  $\tilde{D}_{P'}$  has its inverse. From our experiences this requirement is usually satisfied without any special treatments as long as the transformation includes the rotation as in the case of the angular momentum projection. While a problem may occurs if the two wave functions  $|\Phi\rangle$  and  $|\Phi'\rangle$  have different symmetries, the rotation strongly mixes them and the rank of matrix  $\tilde{D}_{P'}$  does not usually reduce. By using the property in Eq. (48), the contractions for the original basis can be calculated as follows;

$$\rho_{D}^{(c)} = \tau_{Dp'} \rho_{Dp'p}^{(b)} \eta_{p}^{\dagger} = DW'_{p'} \tilde{D}_{P'}^{-1} \rho_{Dp'p}^{(b)} W_{p}^{\dagger}, 
\kappa_{D}^{(c)} = \tau_{Dp'} \kappa_{Dp'p'}^{(b)} \tau_{Dp'}^{T} = DW'_{p'} \tilde{D}_{P'}^{-1} \kappa_{Dp'p'}^{(b)} D_{P'}^{-T} W'_{p'}^{T} D^{T}, 
\bar{\kappa}_{D}^{(c)} = \eta_{p}^{*} \bar{\kappa}_{Dpp}^{(b)} \eta_{p}^{\dagger} = W_{p}^{*} \bar{\kappa}_{Dpp}^{(b)} W_{p}^{\dagger},$$
(51)

where a  $M \times L_{p'}$  matrix  $\tau_{Dp'}$  and a  $M \times L_p$  matrix  $\eta_p$  are defined by

$$\tau_{Dp'} \equiv W \tilde{\tau}_{Dp'} = D W'_{p'} \tilde{D}_{P'}^{-1}, \quad \eta_p \equiv W_p.$$
 (52)

The reduced contractions for the  $(\hat{b}^{\dagger}, \hat{b})$  basis in Eq. (51) are nothing else but their  $L_{p'} \times L_p$ ,  $L_{p'} \times L_{p'}$ , and  $L_p \times L_p$  submatrices, respectively;

$$\rho_{Dp'p}^{(b)} \equiv \left( (\rho_D^{(b)})_{kk'}; k = 1, 2, ..., L_{p'}, k' = 1, 2, ..., L_p \right), 
\kappa_{Dp'p'}^{(b)} \equiv \left( (\kappa_D^{(b)})_{kk'}; k, k' = 1, 2, ..., L_{p'} \right), 
\bar{\kappa}_{Dpp}^{(b)} \equiv \left( (\bar{\kappa}_D^{(b)})_{kk'}; k, k' = 1, 2, ..., L_p \right),$$
(53)

which can be evaluated within the P space. This is because they are more explicitly written as,

$$\bar{\kappa}_{Dpp}^{(b)} = \left[1 + Z_{pp}^{\dagger} Z_{Dpp}^{\prime}\right]^{-1} Z_{pp}^{\dagger}, \quad \rho_{Dp'p}^{(b)} = Z_{Dp'p}^{\prime} \bar{\kappa}_{Dpp}^{(b)}, \quad \kappa_{Dp'p'}^{(b)} = Z_{Dp'p'}^{\prime} - Z_{Dp'p}^{\prime} \bar{\kappa}_{Dpp}^{(b)} Z_{Dpp'}^{\prime},$$

$$(54)$$

where the subblock matrices of  $Z'_D$  are defined by

$$Z'_{Dp'p'} \equiv ((Z'_{D})_{kk'}; k, k' = 1, 2, ..., L_{p'}) = \tilde{D}_{P'} Z'_{p'p'} \tilde{D}_{P'}^{T},$$

$$Z'_{Dp'p} \equiv ((Z'_{D})_{kk'}; k = 1, 2, ..., L_{p'}, k' = 1, 2, ..., L_{p}) = \tilde{D}_{P'} Z'_{p'p'} \tilde{D}_{pp'}^{T},$$

$$Z'_{Dpp'} \equiv ((Z'_{D})_{kk'}; k = 1, 2, ..., L_{p}, k' = 1, 2, ..., L_{p'}) = \tilde{D}_{pp'} Z'_{p'p'} \tilde{D}_{P'}^{T}.$$
(55)

It is now clear that the matrix  $\tilde{D}_{P'}$  and its inverse appearing in the matrix  $\tau_{Dp'}$  in Eq. (52) are auxiliary and introduced just for the sake of convenience of calculation. In fact it is confirmed by Eqs. (51), (54), and (55) that the basic contractions for the original basis  $(\hat{c}^{\dagger}, \hat{c})$  are independent of them.

With these basic contractions for the  $(\hat{b}^{\dagger}, \hat{b})$  basis, overlaps of arbitrary one-body operators can be easily calculated. For the particle-hope (p-h) type operator,  $\hat{F}$ , and particle-particle (p-p) or hole-hole (h-h) type operator,  $\hat{G}^{\dagger}$  or  $\hat{G}$ ,

$$\hat{F} = \sum_{l_1 l_2} F_{l_1 l_2} \hat{c}_{l_1}^{\dagger} \hat{c}_{l_2}, \qquad \hat{G}^{\dagger} = \frac{1}{2} \sum_{l_1 l_2} G_{l_1 l_2} \hat{c}_{l_1}^{\dagger} \hat{c}_{l_2}^{\dagger}, \tag{56}$$

with antisymmetric matrix elements  $G^T = -G$ ,

$$\langle \Phi | \hat{F}[\hat{D}] | \Phi' \rangle = \text{Tr} \{ \rho_{D}^{(c)} F \} = \text{Tr} \{ \rho_{Dp'p}^{(b)} F_{D}^{pp'} \},$$

$$\langle \Phi | \hat{G}[\hat{D}] | \Phi' \rangle = \frac{1}{2} \text{Tr} \{ \kappa_{D}^{(c)} G^{\dagger} \} = \frac{1}{2} \text{Tr} \{ \kappa_{Dp'p'}^{(b)} \bar{G}_{D}^{p'p'} \},$$

$$\langle \Phi | \hat{G}^{\dagger}[\hat{D}] | \Phi' \rangle = \frac{1}{2} \text{Tr} \{ \bar{\kappa}_{D}^{(c)} G \} = \frac{1}{2} \text{Tr} \{ \bar{\kappa}_{Dpp}^{(b)} G^{pp} \},$$
(57)

where the P space matrix elements for  $\hat{F}$ ,  $\hat{G}^{\dagger}$  and  $\hat{G}$  are defined by using the quantities in Eq. (52),

$$F_D^{pp'} \equiv \eta_p^{\dagger} F \tau_{Dp'} = W_p^{\dagger} F D W_{p'}^{\prime} \tilde{D}_{P'}^{-1},$$

$$\bar{G}_D^{p'p'} \equiv \tau_{Dp'}^T G^{\dagger} \tau_{Dp'} = \tilde{D}_{P'}^{-T} W_{p'}^{\prime T} D^T G^{\dagger} D W_{p'}^{\prime} \tilde{D}_{P'}^{-1},$$

$$G^{pp} \equiv \eta_p^{\dagger} G \eta_p^* = W_p^{\dagger} G W_p^*.$$
(58)

In the actual applications of the angular momentum projection, the operator is a spherical tensor, e.g.,  $\hat{G}^{\dagger} = \hat{G}^{\dagger}_{\lambda\mu}$ , and its matrix elements in the original basis satisfy

$$D^{T}(\omega)G^{\dagger}_{\lambda\mu}D(\omega) = \sum_{\mu'} D^{\lambda}_{\mu\mu'}(\omega) G^{\dagger}_{\lambda\mu'}, \tag{59}$$

where  $D^{\lambda}_{\mu\mu'}(\omega)$  is the Wigner *D*-function, and then

$$(\bar{G}_{\lambda\mu})_{D}^{p'p'} = \sum_{\mu'} D_{\mu\mu'}^{\lambda}(\omega) \, \tilde{D}_{P'}^{-T} (G_{\lambda\mu'}^{p'p'})^{\dagger} \tilde{D}_{P'}^{-1}, \quad G_{\lambda\mu}^{p'p'} \equiv W_{p'}^{\dagger} G_{\lambda\mu} W_{p'}^{\prime*}, \tag{60}$$

which can be calculated within the P space. The task is to evaluate the overlap at each integration mesh point in the parameter space, which requires  $O(M^3)$  operations (matrix multiplications) for one-body operators in the original basis. Now it reduces to  $O(ML_p^2)$  for the p-h type operator  $\hat{F}$  and  $O(L_p^3)$  for the p-p or h-h operator  $\hat{G}^{\dagger}$  or  $\hat{G}$  in the truncation scheme  $(L_p \sim L_{p'})$ .

In this paper, we employ separable type schematic interactions. By using the generalized Wick Theorem, we have, for the p-h type interaction,

$$\langle \Phi | : \hat{F}_{1}\hat{F}_{2} : [\hat{D}] | \Phi' \rangle = \operatorname{Tr}\{\rho_{D}^{(c)}F_{1}\}\operatorname{Tr}\{\rho_{D}^{(c)}F_{2}\} - \operatorname{Tr}\{\rho_{D}^{(c)}F_{1}\rho_{D}^{(c)}F_{2}\} + \operatorname{Tr}\{\bar{\kappa}_{D}^{(c)}F_{1}\kappa_{D}^{(c)}F_{2}^{T}\}$$

$$= \operatorname{Tr}\{\rho_{Dp'p}^{(b)}F_{1D}^{pp'}\}\operatorname{Tr}\{\rho_{Dp'p}^{(b)}F_{2D}^{pp'}\}$$

$$-\operatorname{Tr}\{\rho_{Dp'p}^{(b)}F_{1D}^{pp'}\rho_{Dp'p}^{(b)}F_{2D}^{pp'}\} + \operatorname{Tr}\{\bar{\kappa}_{Dpp}^{(b)}F_{1D}^{pp'}\kappa_{Dp'p}^{(b)}F_{2D}^{pp'T}\}, \tag{61}$$

where : : denotes the normal ordering, and for the p-p or h-h type interaction,

$$\langle \Phi | \hat{G}_{1}^{\dagger} \hat{G}_{2}[\hat{D}] | \Phi' \rangle = \frac{1}{4} \left[ \text{Tr} \{ \bar{\kappa}_{D}^{(c)} G_{1} \} \text{Tr} \{ \kappa_{D}^{(c)} G_{2}^{\dagger} \} + 2 \text{Tr} \{ \rho_{D}^{(c)} G_{1} \rho_{D}^{(c)T} G_{2}^{\dagger} \} \right]$$

$$= \frac{1}{2} \text{Tr} \{ \bar{\kappa}_{Dpp}^{(b)} G_{1}^{pp} \} \frac{1}{2} \text{Tr} \{ \kappa_{Dp'p'}^{(b)} \bar{G}_{2D}^{p'p'} \} + \frac{1}{2} \text{Tr} \{ \rho_{Dp'p}^{(b)} G_{1}^{pp} \rho_{Dp'p}^{(b)T} \bar{G}_{2D}^{p'p'} \}. \quad (62)$$

Thus, the basic number of operations to calculate the overlap of the separable type interactions is essentially the same as those of one-body operators, and can be evaluated much faster than the generic two-body interaction (as long as the number of the separable force components are not so large).

For the generic two-body interaction, there are four single-particle indices with two density matrices  $\rho$  or with two pairing tensors  $\kappa$  and  $\bar{\kappa}$ . As is shown in Eq. (51), the two among the four indices are accompanied with the rotation matrix D, and therefore the reduction of the number of operations from  $O(M^4)$  to  $O(M^2L_p^2)$  is expected.

# E. Truncation with respect to particle-hole vacuum

As it is demonstrated in the previous subsection, the use of the Thouless amplitude with respect to the nucleon vacuum, Eq. (35), allows us to dramatically reduce the number of dimension of matrices in the calculation. However, the problem occurs if one takes a limit of vanishing pairing correlations. This is because the amplitude  $U \to 0$  for the hole (occupied) orbits in the limit, and then the Thouless amplitude Z diverges. Moreover, the Thouless form in Eq. (3) can be applied only for the case where the HFB type states  $|\Phi\rangle$  and  $|\Phi'\rangle$  are not orthogonal to the nucleon vacuum, i.e., for the ground states of even-even nuclei. In order to avoid these problems and to generalize the formulation, we introduce the Thouless amplitude with respect to the p-h vacuum (Slater determinant) in place of the nucleon vacuum. Although this makes the formulation more complicated, we have an additional merit; the contribution of core composed of the fully occupied orbits, whose occupation probability is almost one, can be separated and the amount of calculation is further reduced. This effect is considerable especially for heavy nuclei.

Thus, for the two HFB type states  $|\Phi\rangle$  and  $|\Phi'\rangle$ , we introduce the particle-hole vacuums (Slater determinants), which are composed of N canonical-like basis orbits with highest occupation probabilities,

$$|\phi\rangle = \prod_{k=1}^{N} \hat{b}_{k}^{\dagger} | \rangle, \qquad |\phi'\rangle = \prod_{k=1}^{N} \hat{b}_{k}^{\prime \dagger} | \rangle,$$
 (63)

where N is the particle (neutron or proton) number. Note that the index of the canonicallike bases,  $(\hat{b}_i^{\dagger}, \hat{b}_i)$  and  $(\hat{b}_i'^{\dagger}, \hat{b}_i')$ , introduced in the previous subsections, Eqs. (15) and (16), is in descending order of the occupation probabilities. Therefore,  $|\Phi\rangle \to |\phi\rangle$  and  $|\Phi'\rangle \to |\phi'\rangle$ in the limit of vanishing pairing correlations, if the two states  $|\Phi\rangle$  and  $|\Phi'\rangle$  are normalized and their phases are suitably chosen. More precisely, when there exists an unbroken symmetry, e.g., the parity, the N hole orbits should be chosen so that the states  $|\Phi\rangle$  and  $|\phi\rangle$  ( $|\Phi'\rangle$  and  $|\phi'\rangle$ ) belong to the same symmetry representation. Corresponding to the p-h vacuums in Eq. (63), the canonical particle-hole operators  $(\hat{a}^{\dagger}, \hat{a})$ , which satisfy

$$\hat{a}_k |\phi\rangle = 0 \quad (k = 1, 2, ..., M), \qquad \hat{a}'_k |\phi'\rangle = 0 \quad (k = 1, 2, ..., M),$$
 (64)

are defined by

$$a_{k}^{\dagger} = \begin{cases} b_{k} & (1 \le k \le N) \\ b_{k}^{\dagger} & (N+1 \le k \le M) \end{cases}, \qquad a_{k}^{\prime \dagger} = \begin{cases} b_{k}^{\prime} & (1 \le k \le N) \\ b_{k}^{\prime \dagger} & (N+1 \le k \le M) \end{cases}. \tag{65}$$

The relations between these particle-hole bases and the original basis  $(\hat{c}^{\dagger}, \hat{c})$  are given by general Bogoliubov transformations,

$$\hat{a}_{k}^{\dagger} = \sum_{l} \left[ (u_{a})_{lk} \hat{c}_{l}^{\dagger} + (v_{a})_{lk} \hat{c}_{l} \right], \quad \hat{a}_{k}^{\prime \dagger} = \sum_{l} \left[ (u_{a}^{\prime})_{lk} \hat{c}_{l}^{\dagger} + (v_{a}^{\prime})_{lk} \hat{c}_{l} \right], \tag{66}$$

where the Bogoliubov amplitudes  $(u_a, v_a)$  and  $(u'_a, v'_a)$  are simply given by W and W' matrices but specified by the following particle-hole block structure,

$$\begin{cases}
 u_a = \begin{pmatrix} 0 & W_m \end{pmatrix} \\
 v_a = \begin{pmatrix} W_{i}^* & 0 \end{pmatrix}
\end{cases}, \qquad
\begin{cases}
 u'_a = \begin{pmatrix} 0 & W'_{m'} \end{pmatrix} \\
 v'_a = \begin{pmatrix} W'_{i'} & 0 \end{pmatrix}
\end{cases}, \tag{67}$$

where  $W_i$  and  $W'_{i'}$  are the hole part of matrices and of  $M \times N$ , while  $W_m$  and  $W'_{m'}$  are the particle part of matrices and of  $M \times (M-N)$ . This particle-hole decomposition should not be confused with the P and Q space decomposition in Eq. (18), and inequalities  $N \leq L_p$  and  $N \leq L_{p'}$  should be satisfied.

Now we assume that the HFB type states are normalized, and define their Thouless forms with respect to the p-h vacuums. In this subsection we change the notation, and use Z for the Thouless amplitudes for this representation:

$$|\Phi\rangle = n \exp\left[\sum_{k < k'} Z_{kk'} \hat{a}_k^{\dagger} \hat{a}_{k'}^{\dagger}\right] |\phi\rangle, \qquad |\Phi'\rangle = n' \exp\left[\sum_{k < k'} Z'_{kk'} \hat{a}_k'^{\dagger} \hat{a}'_{k'}^{\dagger}\right] |\phi'\rangle. \tag{68}$$

The Thouless amplitudes and the normalization constants in this representation are calculated by

$$Z = (V_a U_a^{-1})^*, \qquad Z' = (V_a' U_a'^{-1})^*,$$

$$(69)$$

$$n = e^{i\theta} \left( \det U_a^* \right)^{1/2}, \qquad n' = e^{i\theta'} \left( \det U_a'^* \right)^{1/2},$$
 (70)

through the Bogoliubov amplitudes  $(U_a, V_a)$  between the quasiparticle basis  $(\hat{\beta}^{\dagger}, \hat{\beta})$  and the p-h basis  $(\hat{a}^{\dagger}, \hat{a})$ ,

$$\hat{\beta}_{k}^{\dagger} = \sum_{k'} \left[ (U_{a})_{k'k} \hat{a}_{k'}^{\dagger} + (V_{a})_{k'k} \hat{a}_{k'} \right], \qquad \hat{\beta}_{k}^{\prime \dagger} = \sum_{k'} \left[ (U_{a}')_{k'k} \hat{a}_{k'}^{\prime \dagger} + (V_{a}')_{k'k} \hat{a}_{k'}^{\prime} \right], \tag{71}$$

and they are written as

$$U_a = \begin{pmatrix} W_i^T V \\ W_m^{\dagger} U \end{pmatrix}, \quad V_a = \begin{pmatrix} W_i^{\dagger} U \\ W_m^T V \end{pmatrix}, \quad U_a' = \begin{pmatrix} W_{i'}^{\prime T} V' \\ W_{m'}^{\prime \dagger} U' \end{pmatrix}, \quad V_a' = \begin{pmatrix} W_{i'}^{\prime \dagger} U' \\ W_{m'}^{\prime T} V' \end{pmatrix}, \quad (72)$$

where (U,V) and (U',V') are the Bogoliubov amplitudes with respect to the original basis  $(\hat{c}^{\dagger},\hat{c})$  for  $|\Phi\rangle$  and  $|\Phi'\rangle$ , respectively. As it clear from Eq. (72),  $U_aU_a^{\dagger} \to 1$ ,  $V_a^*V_a^T \to 0$  for all orbits in the limit of no pairing correlations, and then the Thouless amplitude in this representation does not diverge but vanishes,  $Z \to 0$ . The same is true for Z' and  $|\Phi'\rangle$ .

The transformation between the two p-h bases  $(\hat{a}^{\dagger}, \hat{a})$  and  $(\hat{a}'^{\dagger}, \hat{a}')$  induced by the symmetry operation  $\hat{D}$  is also given by a general Bogoliubov transformation,

$$\hat{D}\hat{a}_{k'}^{\dagger}\hat{D}^{\dagger} = \sum_{k} \left[ (X_D)_{kk'} \hat{a}_k^{\dagger} + (Y_D)_{kk'} \hat{a}_k \right], \tag{73}$$

with the amplitudes defined by

$$X_{D} \equiv u_{a}^{\dagger} D u_{a'}' + v_{a}^{\dagger} D^{*} v_{a'}' = \begin{pmatrix} \tilde{D}_{ii'}^{*} & 0 \\ 0 & \tilde{D}_{mm'} \end{pmatrix},$$

$$Y_{D} \equiv v_{a}^{T} D u_{a'}' + u_{a}^{T} D^{*} v_{a'}' = \begin{pmatrix} 0 & \tilde{D}_{im'} \\ \tilde{D}_{mi'}^{*} & 0 \end{pmatrix},$$
(74)

where the matrix  $\tilde{D}$  is the same as that in Eq. (38) but divided into the p-h block form,

$$\tilde{D} \equiv W^{\dagger}DW' = \begin{pmatrix} W_i^{\dagger}DW_{i'}' & W_i^{\dagger}DW_{m'}' \\ W_m^{\dagger}DW_{i'}' & W_m^{\dagger}DW_{m'}' \end{pmatrix} \equiv \begin{pmatrix} \tilde{D}_{ii'} & \tilde{D}_{im'} \\ \tilde{D}_{mi'} & \tilde{D}_{mm'} \end{pmatrix}.$$
(75)

Combining Eqs. (71) and (73), the transformed quasiparticle operator for the state  $\hat{D}|\Phi'\rangle$  is expressed as

$$\hat{D}\hat{\beta}_{k}^{\prime\dagger}\hat{D}^{\dagger} = \sum_{k'} \left[ (U_{aD}')_{k'k}\hat{a}_{k'}^{\dagger} + (V_{aD}')_{k'k}\hat{a}_{k'} \right], \tag{76}$$

with

$$U'_{aD} = X_D U'_a + Y_D^* V'_a = [X_D^* + Y_D Z']^* U'_a,$$

$$V'_{aD} = X_D^* V'_a + Y_D U'_a = [X_D Z' + Y_D^*]^* U'_a,$$
(77)

from which the Thouless form of the transformed state is obtained;

$$\hat{D}|\Phi'\rangle = n' e^{i\Theta(\hat{D})} \left( \det(U'_{aD} U'^{-1}_{a})^* \right)^{1/2} \exp \left[ \sum_{k < k'} (Z'_{D})_{kk'} \hat{a}_{k}^{\dagger} \hat{a}_{k'}^{\dagger} \right] |\phi\rangle, \tag{78}$$

where the phase  $\Theta(\hat{D})$  coming from the transformation is introduced in Eqs. (12) and (13), and the new Thouless amplitude  $Z'_D$  is defined by

$$Z_D' \equiv \left(V_{aD}'U_{aD}'^{-1}\right)^* = \left[X_D Z' + Y_D^*\right] \left[X_D^* + Y_D Z'\right]^{-1}.$$
 (79)

Introducing two new antisymmetric matrices,

$$S_D^{\dagger} \equiv X_D^{-*} Y_D = -S_D^*, \qquad \tilde{S}_D \equiv (Y_D X_D^{-1})^* = -\tilde{S}_D^T,$$
 (80)

the Thouless amplitude of the transformed state in Eq. (79) can be written as

$$Z_D' = X_D^{-\dagger} Z' \left[ 1 + S_D^{\dagger} Z' \right]^{-1} X_D^{-*} + \tilde{S}_D, \tag{81}$$

and the norm overlap is calculated as

$$\langle \Phi | \hat{D} | \Phi' \rangle = n^* n' e^{i\Theta(\hat{D})} \left( \det \left[ X_D^* + Y_D Z' \right] \right)^{1/2} \left( \det \left[ 1 + Z^{\dagger} Z_D' \right] \right)^{1/2} 
= n^* n' e^{i\Theta(\hat{D})} \left( \det X_D^* \right)^{1/2} \left( \det \left[ 1 + S_D^{\dagger} Z' \right]_{p'p'} \right)^{1/2} \left( \det \left[ 1 + Z^{\dagger} Z_D' \right]_{pp} \right)^{1/2} 
= n^* n' \langle \phi | \hat{D} | \phi' \rangle (-1)^{L_{p'}(L_{p'}+1)/2} (-1)^{L_p(L_p+1)/2} 
\times \operatorname{pf} \left( Z'_{p'p'} - 1 \atop 1 S_{Dp'p'}^{\dagger} \right) \operatorname{pf} \left( Z'_{Dpp} - 1 \atop 1 Z_{pp}^{\dagger} \right), \tag{82}$$

where the following identity for the norm overlap for the p-h vacuums is used;

$$e^{i\Theta(\hat{D})} \left(\det X_D^*\right)^{1/2} = \langle \phi | \hat{D} | \phi' \rangle. \tag{83}$$

Taking into account the fact that

$$Z'_{Dpp} = (X_D^{-\dagger})_{pp'} Z'_{p'p'} \left[ 1 + S^{\dagger}_{Dp'p'} Z'_{p'p'} \right]^{-1} (X_D^{-*})_{p'p} + \tilde{S}_{Dpp}, \tag{84}$$

the norm overlap in Eq. (82) can be calculated within the P space, if the quantities  $(X_D^{-1})_{pp'}$ ,  $\tilde{S}_{Dp'p'}$ ,  $\tilde{S}_{Dpp}$ , and  $\langle \phi | \hat{D} | \phi' \rangle$  can be calculated easily. This is actually the case, because their explicit forms can be written as

$$X_D^{-1} = \begin{pmatrix} \tilde{D}_{ii'}^{-*} & 0\\ 0 & \tilde{D}_{mm'}^{-1} \end{pmatrix} = \begin{pmatrix} \tilde{D}_{ii'}^{-*} & 0\\ 0 & \tilde{D}_{mm'}^{\dagger} - \tilde{D}_{im'}^{\dagger} \tilde{D}_{ii'}^{-\dagger} \tilde{D}_{mi'}^{\dagger} \end{pmatrix}, \tag{85}$$

$$S_D^{\dagger} = \begin{pmatrix} 0 & \tilde{D}_{ii'}^{-1} \tilde{D}_{im'} \\ -\tilde{D}_{im'}^T \tilde{D}_{ii'}^{-T} & 0 \end{pmatrix}, \qquad \tilde{S}_D = \begin{pmatrix} 0 & -\tilde{D}_{ii'}^{-T} \tilde{D}_{mi'}^T \\ \tilde{D}_{mi'} \tilde{D}_{ii'}^{-1} & 0 \end{pmatrix}, \tag{86}$$

and

$$\langle \phi | \hat{D} | \phi' \rangle = \det \tilde{D}_{ii'},$$
 (87)

so that the matrix manipulations are confined in the hole space, which is smaller than (or equal to) the P space.

As for the contractions, those for the p-h basis  $(\hat{a}^{\dagger}, \hat{a})$  can be calculated in terms of the new Thouless amplitudes introduced in this subsection, Z and  $Z'_D$  in Eqs. (68) and (78), as

$$\begin{pmatrix} \rho_D^{(a)} \end{pmatrix}_{k'k} \equiv \langle \Phi | \hat{a}_k^{\dagger} \hat{a}_{k'} [\hat{D}] | \Phi' \rangle = \left( Z_D' \left[ 1 + Z^{\dagger} Z_D' \right]^{-1} Z^{\dagger} \right)_{k'k}, 
\left( \kappa_D^{(a)} \right)_{k'k} \equiv \langle \Phi | \hat{a}_k \hat{a}_{k'} [\hat{D}] | \Phi' \rangle = \left( Z_D' \left[ 1 + Z^{\dagger} Z_D' \right]^{-1} \right)_{k'k}, 
\left( \bar{\kappa}_D^{(a)} \right)_{k'k} \equiv \langle \Phi | \hat{a}_k^{\dagger} \hat{a}_{k'}^{\dagger} [\hat{D}] | \Phi' \rangle = \left( \left[ 1 + Z^{\dagger} Z_D' \right]^{-1} Z^{\dagger} \right)_{k'k}.$$
(88)

Their structures in terms of Z and  $Z'_D$  matrices are the same as those for the  $(\hat{b}^{\dagger}, \hat{b})$  basis in the previous subsection. Namely,  $\bar{\kappa}_D^{(a)}$  has the same block form as in Eq. (45), and the same identities as in Eq. (46) hold. Therefore, their reduced contractions,

$$\rho_{Dp'p}^{(a)} \equiv \left( (\rho_D^{(a)})_{kk'}; \ k = 1, 2, ..., L_{p'}, k' = 1, 2, ..., L_p \right), 
\kappa_{Dp'p'}^{(a)} \equiv \left( (\kappa_D^{(a)})_{kk'}; \ k, k' = 1, 2, ..., L_{p'} \right), 
\bar{\kappa}_{Dpp}^{(a)} \equiv \left( (\bar{\kappa}_D^{(a)})_{kk'}; \ k, k' = 1, 2, ..., L_p \right),$$
(89)

can be evaluated within the P space. By using the definition in Eq. (65), the contractions for the  $(\hat{b}^{\dagger}, \hat{b})$  basis are related to those for the  $(\hat{a}^{\dagger}, \hat{a})$  basis;

$$\rho_D^{(b)} = \begin{pmatrix} 1_{ii} - \rho_{Dii}^{(a)T} & \bar{\kappa}_{Dim}^{(a)} \\ \kappa_{Dmi}^{(a)} & \rho_{Dmm}^{(a)} \end{pmatrix}, \quad \kappa_D^{(b)} = \begin{pmatrix} \bar{\kappa}_{Dii}^{(a)} & -\rho_{Dmi}^{(a)T} \\ \rho_{Dmi}^{(a)} & \kappa_{Dmm}^{(a)} \end{pmatrix}, \quad \bar{\kappa}_D^{(b)} = \begin{pmatrix} \kappa_{Dii}^{(a)} & \rho_{Dim}^{(a)} \\ -\rho_{Dim}^{(a)T} & \bar{\kappa}_{Dmm}^{(a)} \end{pmatrix}, \quad (90)$$

where  $1_{ii}$  is the  $N \times N$  unit matrix. These basic contractions can be calculated also within the P space. Thus, the contractions for the original basis are obtained as in Eq. (51) in the previous subsection, and so are the overlaps of arbitrary observables; i.e., most of their calculations can be performed within the P space.

Now we discuss the method to further reduce the calculation by taking account of the core contributions, where the core means the subspace composed of the canonical orbits which have almost full occupation probability,  $v^2 \approx 1$ , (deep hole states). More precisely,

setting up a small number  $\epsilon$ , we select the core space O composed of the canonical orbits which satisfy  $u_k^2 = 1 - v_k^2 < \epsilon$ ,  $k = 1, 2, ..., L_o(\epsilon)$ , for  $|\Phi\rangle$  and,  $u_k'^2 = 1 - v_k'^2 < \epsilon$ ,  $k = 1, 2, ..., L_{o'}(\epsilon)$ , for  $|\Phi'\rangle$ , respectively, in a similar manner as selecting the P space. Namely, the p-h bases satisfy (omitting  $(\epsilon)$  in  $L_o(\epsilon)$  and  $L_{o'}(\epsilon)$ )

$$\hat{a}_k |\Phi\rangle = 0, \quad k \le L_o, \qquad \hat{a}'_{k'} |\Phi'\rangle = 0, \quad k' \le L_{o'}.$$
 (91)

Note that the core subspace O is contained in the P space,  $P=O \oplus \bar{P}$ , and inequalities  $0 \le L_o \le N \le L_p \le M$  and  $0 \le L_{o'} \le N \le L_{p'} \le M$  hold. The dimensions of the non-zero Thouless amplitudes for the p-h bases in Eq. (68) are then further reduced,

$$Z_{pp} = \begin{pmatrix} 0 & 0 \\ 0 & Z_{\bar{p}\bar{p}} \end{pmatrix}, \qquad Z'_{p'p'} = \begin{pmatrix} 0 & 0 \\ 0 & Z'_{\bar{p}'\bar{p}'} \end{pmatrix},$$
 (92)

and then

$$Z'_{Dpp} = (X_D^{-\dagger})_{p\bar{p}'} Z'_{\bar{p}'\bar{p}'} \left[ 1 + S^{\dagger}_{D\bar{p}'\bar{p}'} Z'_{\bar{p}'\bar{p}'} \right]^{-1} (X_D^{-*})_{\bar{p}'p} + \tilde{S}_{Dpp}, \tag{93}$$

where the submatrix  $(X_D^{-\dagger})_{p\bar{p}'}$  is defined by

$$(X_D^{-\dagger})_{p\bar{p}'} \equiv ((X_D^{-\dagger})_{kk'}; k = 1, 2, ..., L_p, k' = L_{o'} + 1, L_{o'} + 2, ..., L_{p'}), \tag{94}$$

and the sizes of square submatrices  $Z_{\bar{p}\bar{p}}$  and  $Z_{\bar{p}'\bar{p}'}$  in the  $\bar{P}$  space are  $L_{\bar{p}} \equiv L_p - L_o$  and  $L_{\bar{p}'} \equiv L_{p'} - L_{o'}$ , respectively. Then the calculation of the norm overlap in Eq. (82) is further reduced in such a way that the determinants or the pfaffians have smaller sizes  $L_p \to L_{\bar{p}}$  and  $L_{p'} \to L_{\bar{p}'}$ . As for the contractions, although the reductions of the dimensions of matrix manipulation are restrictive, their effect is still considerable.

From Eq. (92), the reduced contraction  $\bar{\kappa}_{Dpp}^{(a)}$  has a subblock form,

$$\bar{\kappa}_{Dpp}^{(a)} = \begin{pmatrix} 0 & 0 \\ 0 & [1 + Z_{\bar{p}\bar{p}}^{\dagger} Z_{D\bar{p}\bar{p}}']^{-1} Z_{\bar{p}\bar{p}}^{\dagger} \end{pmatrix} \equiv \begin{pmatrix} 0 & 0 \\ 0 & \bar{\kappa}_{D\bar{p}\bar{p}}^{(a)} \end{pmatrix}, \tag{95}$$

and then

$$\rho_{Dp'p}^{(a)} = \begin{pmatrix} 0 & Z'_{Do\bar{p}}\bar{\kappa}_{D\bar{p}\bar{p}}^{(a)} \\ 0 & Z'_{D\bar{p}'\bar{p}}\bar{\kappa}_{D\bar{p}\bar{p}}^{(a)} \end{pmatrix}, \qquad \kappa_{Dp'p'}^{(a)} = Z'_{Dp'p'} - Z'_{Dp'\bar{p}}\bar{\kappa}_{D\bar{p}\bar{p}}^{(a)} Z'_{D\bar{p}p'}, \tag{96}$$

where the subblock matrices of  $Z'_D$  are defined obviously by

$$Z'_{Do\bar{p}} \equiv ((Z'_{D})_{kk'}; k = 1, 2, ..., L_{o}, k' = L_{o} + 1, L_{o} + 2, ..., L_{p}),$$

$$Z'_{D\bar{p}'\bar{p}} \equiv ((Z'_{D})_{kk'}; k = L_{o} + 1, L_{o} + 2, ..., L_{p'}, k' = L_{o} + 1, L_{o} + 2, ..., L_{p}),$$

$$Z'_{Dp'\bar{p}} \equiv ((Z'_{D})_{kk'}; k = 1, 2, ..., L_{p'}, k' = L_{o} + 1, L_{o} + 2, ..., L_{p}),$$

$$Z'_{D\bar{p}p'} \equiv ((Z'_{D})_{kk'}; k = L_{o} + 1, L_{o} + 2, ..., L_{p}, k' = 1, 2, ..., L_{p'}).$$

$$(97)$$

Namely, non-zero part of  $\bar{\kappa}_D^{(a)}$  is reduced from  $L_p \times L_p$  to  $L_{\bar{p}} \times L_{\bar{p}}$ , that of  $\rho_{Dp'p}^{(a)}$  from  $L_{p'} \times L_p$  to  $L_{p'} \times L_{\bar{p}}$ , while that of  $\kappa_D^{(a)}$  is unchanged and  $L_{p'} \times L_{p'}$ . Using these contractions and Eq. (90), the basic contractions for the  $(\hat{b}^{\dagger}, \hat{b})$  basis take the following subblock forms,

$$\rho_{Dp'p}^{(b)} = \begin{pmatrix} 1_{oo} & 0\\ \rho_{D\bar{p}'o}^{(b)} & \rho_{D\bar{p}'\bar{p}}^{(b)} \end{pmatrix}, \quad \kappa_{Dp'p'}^{(b)} = \begin{pmatrix} 0 & 0\\ 0 & \kappa_{D\bar{p}'\bar{p}'}^{(b)} \end{pmatrix}, \quad \bar{\kappa}_{Dpp}^{(b)} = \begin{pmatrix} \bar{\kappa}_{Doo}^{(b)} & \bar{\kappa}_{Do\bar{p}}^{(b)}\\ \bar{\kappa}_{D\bar{p}o}^{(b)} & \bar{\kappa}_{D\bar{p}\bar{p}}^{(b)} \end{pmatrix}, \quad (98)$$

where  $1_{oo}$  is the  $L_o \times L_o$  unit matrix. Thus, the overlap calculations of one-body and two-body operators in Eqs. (57), (61), and (62) are considerably reduced, especially for heavy nuclei with weak pairing correlations.

In this way, we have shown that the truncation scheme within the P space works for more general representations based on the p-h vacuums (Slater determinants), although the formula are more complicated. Furthermore, the additional reduction of matrix manipulations is possible related to the core contributions. Various subblocks for the matrix representation of the amplitudes or of observables in the  $(\hat{b}^{\dagger}, \hat{b})$  or  $(\hat{a}^{\dagger}, \hat{a})$  basis are introduced; the P and Q spaces, the particle and hole spaces, and the core space O with  $P = O \oplus \bar{P}$ . They are summarized for the Thouless amplitude Z for the  $(\hat{a}^{\dagger}, \hat{a})$  basis as

$$Z = \begin{pmatrix} i_o & i_{\bar{p}} & m_{\bar{p}} & m_q \\ i_{\bar{p}} & 0 & 0 & 0 \\ 0 & * & * & 0 \\ m_{\bar{p}} & 0 & * & * & 0 \\ 0 & * & * & 0 \\ 0 & 0 & 0 & 0 \end{pmatrix}, \tag{99}$$

where the subindex  $i_o$  denotes the core orbits,  $i_{\bar{p}}$  the remaining hole orbits,  $m_{\bar{p}}$  the particle orbits in the P space, and  $m_q$  the Q space orbits. Their borders are specified by the dimensions,  $L_o$ , N (particle number), and  $L_p$ , respectively, in the full space dimension M.

Finally we mention that the arbitrary phases of the HFB type states in Eq. (70) can be conveniently chosen;

$$n = |\det U_a|^{1/2} = \det \left[ 1 + Z^{\dagger} Z \right]_{\bar{p}\bar{p}}^{-1/4}, \quad n' = |\det U'_{a'}|^{1/2} = \det \left[ 1 + Z'^{\dagger} Z' \right]_{\bar{p}'\bar{p}'}^{-1/4}, \quad (100)$$

which naturally guarantee the condition,  $|\Phi\rangle \to |\phi\rangle$  and  $|\Phi'\rangle \to |\phi'\rangle$  in the limit of vanishing pairing correlations. In this limit, the basic contractions take the forms

$$\rho_{Dp'p}^{(b)} \to 1_{ii}, \qquad \kappa_{Dp'p'}^{(b)} \to 0, \qquad \bar{\kappa}_{Dpp}^{(b)} \to 0,$$
(101)

with which the formula for the quantum number projection (and/or the configuration mixing) for the Slater determinantal states are recovered.

## III. EXAMPLE CALCULATIONS

#### A. Choice of Hamiltonian

In this section, we show some examples of the result of calculations, which are obtained by applying the formulation developed in the previous section. It is required to start with the spherically invariant two-body Hamiltonian. Although it is desirable to use realistic interactions like the Gogny or Skyrme forces, it has been recognized that the density-dependent part of interaction causes some problems for the quantum number projection and/or the configuration mixing calculations; see e.g. Refs. [30–32]. In this paper, we restrict ourselves to the schematic multipole-multipole two-body interactions for simplicity. However, in order to make the result as realistic as possible, we employ the Woods-Saxon potential as a mean-field, and construct the residual multipole interactions consistent with it according to Ref. [7]. Needless to say, the Hamiltonian is spherical invariant; therefore, we start from a hypothetical spherical ground state for the construction.

Thus, our Hamiltonian is written as

$$\hat{H} = \hat{h} + \hat{H}_F + \hat{H}_G, \qquad \hat{h} = \hat{h}_0 + \hat{h}_1, \qquad \hat{h}_0 = \sum_{\tau = n, n} \left( \hat{t}_\tau + \hat{V}_{WS}^\tau \right),$$
 (102)

where  $\hat{h}_0$  is a spherical mean-field Hamiltonian composed of the kinetic energy and the Woods-Saxon potential (with the Coulomb interaction for proton), and  $\tau = n, p$  distinguishes neutron or proton. The part  $\hat{h}_1$  is included to cancel out the exchange contributions coming from the residual interactions  $\hat{H}_F$  and  $\hat{H}_G$ , and is discussed later. Assuming

the same spatial deformation for neutron and proton, the particle-hole type (F-type) isoscalar interaction  $\hat{H}_F$  is given by

$$\hat{H}_F = -\frac{1}{2} \chi \sum_{\lambda \ge 2} \sum_{\mu} (-1)^{\mu} : \hat{F}_{\lambda - \mu} \hat{F}_{\lambda \mu} :, \qquad \hat{F}_{\lambda \mu} = \sum_{\tau = n, p} \hat{F}_{\lambda \mu}^{\tau}, \tag{103}$$

where the operator  $\hat{F}^{\tau}_{\lambda\mu}$ ,

$$\hat{F}_{\lambda\mu}^{\tau} \equiv \sum_{ij} \langle i | \hat{F}_{\lambda\mu}^{\tau} | j \rangle \hat{c}_i^{\dagger} \hat{c}_j, \tag{104}$$

is defined by the one-body field,

$$F_{\lambda\mu}^{\tau}(\mathbf{r}) = R_0^{\tau} \frac{dV_c^{\tau}}{dr} Y_{\lambda\mu}(\theta, \phi), \tag{105}$$

with  $V_c^{\tau}(r)$  and  $R_0^{\tau}$  being the central part of the Woods-Saxon potential and its radius, respectively. As is already mentioned, we employ the spherical harmonic oscillator basis as the original basis states  $\{|i\rangle\}$ . The selfconsistent force parameter  $\chi$  is independent of the multipolarity  $\lambda$  and is given by

$$\chi = (\kappa_n + \kappa_p)^{-1}, \qquad \kappa_\tau \equiv (R_0^\tau)^2 \int \rho_0^\tau(r) \frac{d}{dr} \left( r^2 \frac{dV_c^\tau(r)}{dr} \right) dr, \tag{106}$$

where  $\rho_0^{\tau}(r)$  is the spherical ground state density, which is calculated with the filling approximation for each nucleus based on the spherical Woods-Saxon single-particle state of  $\hat{h}_0$ .

As for the pairing (G-type) interaction  $\hat{H}_G$ ,

$$\hat{H}_G = -\sum_{\tau,\lambda>0} g_{\lambda}^{\tau} \sum_{\mu} \hat{G}_{\lambda\mu}^{\tau\dagger} \hat{G}_{\lambda\mu}^{\tau}, \qquad \hat{G}_{\lambda\mu}^{\tau\dagger} \equiv \frac{1}{2} \sum_{ij} \langle i | \tilde{G}_{\lambda\mu}^{\tau} | j \rangle \hat{c}_i^{\dagger} \hat{c}_{\tilde{j}}^{\dagger}, \tag{107}$$

where  $\tilde{j}$  denotes the time reversal conjugate state of j, we employ the standard multipole form defined by the operator,

$$\tilde{G}_{\lambda\mu}(\mathbf{r}) = \left(\frac{r}{\bar{R}_0}\right)^{\lambda} \sqrt{\frac{4\pi}{2\lambda + 1}} Y_{\lambda\mu}(\theta, \phi), \tag{108}$$

with  $\bar{R}_0 = 1.2A^{1/3}$  fm. Just like the zero-range interactions, this type of simplified pairing interactions cannot be used with the full model space. We employ cut-off of the matrix elements for the operator  $\tilde{G}_{\lambda\mu}^{\tau}$ ; namely the following replacement is done:

$$\langle i|\tilde{G}_{\lambda\mu}^{\tau}|j\rangle \to \sum_{kl} w_{ik}^{0\tau*} w_{jl}^{0\tau} \left[ f_{c}(\epsilon_{k}^{0\tau}) f_{c}(\epsilon_{l}^{0\tau}) \right]^{1/2} \times \langle k|\tilde{G}_{\lambda\mu}^{\tau}|l\rangle_{WS}^{0}, \tag{109}$$

where  $\epsilon_l^{0\tau}$  and  $\langle k|\tilde{G}_{\lambda\mu}^{\tau}|l\rangle_{\rm WS}^0$  are the eigenenergies of the spherical Woods-Saxon states and the matrix elements with respect to them, respectively, and  $w_{ik}^{0\tau}$  is their transformation matrix from the original harmonic oscillator basis states. We use the following form of the cut-off factor [33],

$$f_{\rm c}(\epsilon) = \frac{1}{2} \left[ 1 + \operatorname{erf}\left(\frac{\epsilon - \lambda + \Lambda_{\rm l}}{d_{\rm cut}}\right) \right]^{1/2} \left[ 1 + \operatorname{erf}\left(\frac{-\epsilon + \lambda + \Lambda_{\rm u}}{d_{\rm cut}}\right) \right]^{1/2}, \tag{110}$$

where the error function is defined by  $\operatorname{erf}(x) = \frac{2}{\sqrt{\pi}} \int_0^x e^{-t^2} dt$ , and the parameters are chosen to be  $\Lambda_{\rm u} = \Lambda_{\rm l} = 1.2\,\hbar\omega$  and  $d_{\rm cut} = 0.2\,\hbar\omega$  with  $\hbar\omega = 41/A^{1/3}$  MeV. The quantity  $\lambda$  in the cut-off factor in Eq.(110) is the chemical potential determined to guarantee the correct average number in the treatment of pairing correlation (see the next subsection).

It should be noted that all the two-body terms, including the exchange contributions, are evaluated in the calculation of the quantum number projection. Even for the hypothetical spherical ground state, the exchange term of the interaction  $\hat{H}_F$  and  $\hat{H}_G$  induces extra spherical one-body fields, which are written explicitly as,

$$\hat{h}_F \equiv \chi \sum_{\tau,\lambda \ge 2} \sum_{ij} \left( \sum_{\mu} \sum_{kl} (-1)^{\mu} \langle i | \hat{F}_{\lambda-\mu}^{\tau} | k \rangle (\rho_0^{\tau})_{kl} \langle l | \hat{F}_{\lambda\mu}^{\tau} | j \rangle \right) \hat{c}_i^{\dagger} c_j, \tag{111}$$

and

$$\hat{h}_G \equiv -\sum_{\tau,\lambda>0} g_{\lambda}^{\tau} \sum_{ij} \left( \sum_{\mu} \sum_{kl} \langle il | \hat{G}_{\lambda\mu}^{\tau\dagger} | \rangle (\rho_0^{\tau})_{kl} \langle | \hat{G}_{\lambda\mu}^{\tau} | jk \rangle \right) \hat{c}_i^{\dagger} c_j, \tag{112}$$

where  $(\rho_0^{\tau})_{kl}$  is the density matrix for the spherical ground state. Since the Hamiltonian consists of the one-body part and its residual interaction for the spherical ground state, we subtract these terms from the one-body Hamiltonian  $\hat{h}_0$  and the one-body field  $\hat{h}_1$  in Eq. (102) is given by

$$\hat{h}_1 = -\hat{h}_F - \hat{h}_G. {113}$$

Note that this term  $\hat{h}_1$  is not used to generate the mean-field states from which the projection calculations are performed.

As for the parameter set for the Woods-Saxon potential, we use the one recently proposed by Ramon Wyss [35] and employed in Refs. [33, 36, 37], which very nicely reproduces the geometrical property like the nuclear radius.

#### B. Details of calculation

We have developed a program to perform the general quantum number projection and the configuration mixing for the Hamiltonian in Eq. (102) according to the formulation in Sec. II. We have made the program in such a way that most general symmetry-breaking mean-field states (HFB type states)  $|\Phi\rangle$  can be accepted as long as they are expanded in the spherical harmonic oscillator basis. More precisely, the angular momentum projection, neutron and proton number projections, and the parity projection are performed simultaneously; and, optionally, the configuration mixing in the sense of the GCM can be done. Namely, the final nuclear wave function is expressed as,

$$|\Psi_{M;\alpha}^{INZ(\pm)}\rangle = \sum_{K,n} g_{Kn,\alpha}^{INZ(\pm)} \hat{P}_{MK}^I \hat{P}^N \hat{P}^Z \hat{P}_{\pm} |\Phi_n\rangle. \tag{114}$$

The projectors are given, as usual, by

$$\hat{P}_{MK}^{I} = \frac{2I+1}{8\pi^2} \int d^3\omega D_{MK}^{I*}(\omega) \hat{R}(\omega), \qquad \hat{P}^{N} = \frac{1}{2\pi} \int d\varphi \, e^{i\varphi(\hat{N}-N)}, \tag{115}$$

the similar one for the proton number projector  $\hat{P}^Z$ , and the parity projector  $\hat{P}_{\pm}$  in Eq. (10). The mixing amplitude  $g_{Kn,\alpha}^{INZ(\pm)}$  is obtained by solving the generalized eigenvalue problem of the Hill-Wheeler equation,

$$\sum_{K',n'} \mathcal{H}_{Kn;K'n'}^{INZ(\pm)} g_{K'n',\alpha}^{INZ(\pm)} = E_{\alpha}^{INZ(\pm)} \sum_{K',n'} \mathcal{N}_{Kn;K'n'}^{INZ(\pm)} g_{K'n',\alpha}^{INZ(\pm)}, \tag{116}$$

where the Hamiltonian and norm kernels are defined as

$$\begin{pmatrix} \mathcal{H}_{Kn;K'n'}^{INZ(\pm)} \\ \mathcal{N}_{Kn;K'n'}^{INZ(\pm)} \end{pmatrix} = \langle \Phi_n | \begin{pmatrix} \hat{H} \\ 1 \end{pmatrix} \hat{P}_{KK'}^I \hat{P}^N \hat{P}^Z \hat{P}_{\pm} | \Phi_{n'} \rangle. \tag{117}$$

In the present paper, however, we only show the results of the quantum number projection; namely, no configuration mixing is performed.

The generalized eigenvalue problem in Eq. (116) is solved in a standard way, i.e., the socalled two step method. Namely, first the norm kernel is diagonalized and the states with small norm eigenvalue are discarded, and then the remaining energy eigenvalue problem is solved in the restricted space. In the present work for the general quantum number projections, we have excluded the state whose norm eigenvalue is smaller than  $10^{-13}$ . The numerical integrations for the projectors in Eq. (115) is treated by the standard Gaussian quadratures. It should be noted that since we do not impose any symmetry like  $D_2$  the number of points required for the Gaussian quadratures are considerably large.

As for the mean-field state  $|\Phi\rangle$ , it may be desirable to apply the HFB procedure. However, we found that the schematic separable type interaction in Eq. (102) with large model space does not always gives a reasonable result, e.g., the appropriate ground state deformation. Therefore, in the present work, we utilize the following deformed mean-field Hamiltonian,

$$\hat{h}_{\text{def}} = \hat{h}_0 - \sum_{\lambda \mu} \alpha_{\lambda \mu}^* \hat{F}_{\lambda \mu}, \tag{118}$$

where the deformation parameters  $\{\alpha_{\lambda\mu}\}$  are basically determined by the Woods-Saxon Strutinsky calculation of Ref. [33]. The deformed mean-field in Eq. (118) is obtained from the schematic interaction (103) in the Hartree-Bogoliubov (HB) approximation if the selfconsistent condition,  $\alpha_{\lambda\mu} = \chi \langle \Phi | \hat{F}_{\lambda\mu} | \Phi \rangle$ , is satisfied. At the same time, it coincides, within the first order in the deformation parameters, with the central part of the standard deformed Woods-Saxon potential [34], which is used in Ref. [33]. The potential is defined with respect to the deformed nuclear surface specified by the radius,

$$R(\theta, \phi) = R_0 c_v(\{\alpha_{\lambda\mu}\}) \left[ 1 + \sum_{\lambda\mu} \alpha_{\lambda\mu}^* Y_{\lambda\mu}(\theta, \phi) \right], \qquad (119)$$

where the constant  $c_v(\{\alpha_{\lambda\mu}\})$  takes care of the volume conservation.

With the deformed Hamiltonian in Eq. (118), the mean-field state  $|\Phi\rangle$  is generated by the paired and cranked mean-field,

$$\hat{h}'_{\text{mf}} = \hat{h}_{\text{def}} - \sum_{\tau=\text{n,p}} \Delta_{\tau} \left( \hat{P}_{\tau}^{\dagger} + \hat{P}_{\tau} \right) - \sum_{\tau=\text{n,p}} \lambda_{\tau} \hat{N}_{\tau} - \omega_{\text{rot}} \hat{J}_{x}, \tag{120}$$

where  $\hat{N}_{\tau}$  and  $\lambda_{\tau}$  are the particle number operator and the chemical potential, respectively, while  $\hat{P}_{\tau}^{\dagger} = \hat{G}_{00}^{\tau\dagger}$  and  $\Delta_{\tau} = g_0^{\tau} \langle \Phi | \hat{G}_{00}^{\tau} | \Phi \rangle$ , namely the static monopole pairing part in the Hamiltonian in Eq. (107) is included selfconsistently within the HB procedure to generate the mean-field state  $|\Phi\rangle$ . The ground states of nuclei considered in the present example calculations are axially symmetric,  $\alpha_{\lambda\mu} = 0$  for  $\mu \neq 0$ , and the effect of the rotation about the x-axis perpendicular to the symmetry axis is taken into account with the rotational frequency  $\omega_{\rm rot}$ . We do not intend to study high spin states in the present work, and are mainly concerned about the ground state band. However, we found that the K mixing

caused by the cranking procedure is essential to reproduce the moment of inertia; as will be discussed in the followings, a small cranking frequency is enough for such a purpose.

By using the Woods-Saxon Strutinsky calculation of Ref. [33] the axially symmetric quadrupole and hexadecapole deformations,  $\alpha_{20}$  and  $\alpha_{40}$ , are determined. For parity breaking case, we additionally include  $\alpha_{30}$  deformation in such a way to roughly reproduce the energy splitting of the ground state parity doublet bands. Correspondingly, we include  $\lambda = 2, 3, 4$  components in the isoscalar F-type interactions in Eq. (103) with the common selfconsistent strength  $\chi$  given in Eq. (106). As for the G-type interaction, we include  $\lambda = 0, 2$  components. The monopole pairing ( $\lambda = 0$ ) strength  $g_0^{\tau}$  is determined so that the pairing gap  $\Delta_{\tau}$  at zero frequency  $\omega_{\rm rot} = 0$  in Eq. (120) reproduces the even-odd mass differences. The quadrupole pairing strength is assumed to be proportional to the monopole pairing strength and the proportionality constant, which is assumed to be common to neutron and proton, is chosen to reproduce the final rotational spectra. We assume the constant deformations for the cranking calculation for simplicity. The effects of cranking for the results of angular-momentum-projection calculation are discussed in the following two examples.

# C. Rotational spectrum in <sup>164</sup>Er

As a first example, we consider a typical rotational spectrum of the ground state band in the rare earth region, taking a nucleus <sup>164</sup>Er. The parameters determined according to the procedure explained in the previous subsection and used in the calculation are summarized in Table I. Strictly speaking, the values of the F-type interaction strength  $\chi$  and the monopole pairing interaction strength  $g_0^{\tau}$  depend on the size of the spherical oscillator basis. However, their dependences are very weak if the size is large enough. We present the values for  $N_{\text{osc}}^{\text{max}} = 18$ . In this case the parity of the mean-field is conserved and the parity projection is unnecessary; all the states belong to the positive parity. To perform the angular momentum projection, the numbers of points for the Gaussian quadratures with respect to the Euler angles,  $\omega = (\alpha, \beta, \gamma)$ , are  $N_{\alpha} = N_{\gamma} = 16$  and  $N_{\beta} = 50$  for the non-cranked case and for the case with the small cranking frequency  $\hbar \omega_{\text{rot}} = 0.01$  MeV. For the cases with larger cranking frequencies, they are increased to

 $N_{\alpha} = N_{\gamma} = 22$  and  $N_{\beta} = 70$ . As for the number projection, the number of mesh points with respect to the gauge angle is  $N_{\varphi} = 17$  for both neutron and proton. These values are chosen to guarantee the convergence of the results.

$\alpha_{20}$	$\alpha_{30}$	$\alpha_{40}$	$\chi \; [\mathrm{MeV^{-1}}]$	$\Delta_{\rm n} \; [{ m MeV}]$	$\Delta_{\rm p} \; [{ m MeV}]$	$g_0^{\rm n} \; [{ m MeV}]$	$g_0^{\rm p} \; [{ m MeV}]$	$g_2^{ au}/g_0^{ au}$
0.276	0	0.012	$2.566 \times 10^{-4}$	1.020	1.025	0.1606	0.2096	13.60

TABLE I: The parameters used in the calculation for  $^{164}_{68}\mathrm{Er}_{96}$ . The values of  $\chi$  and  $g_0^{\tau}$  are those with the size of basis  $N_{\mathrm{osc}}^{\mathrm{max}}=18$ .

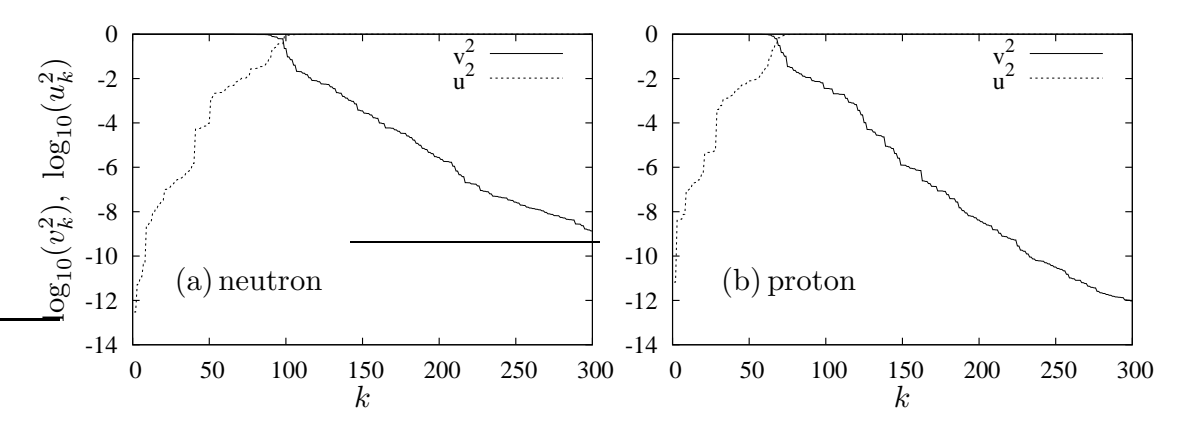


FIG. 1: Occupation and empty probabilities  $v_k^2$  and  $u_k^2 = 1 - v_k^2$  as functions of the number k of the canonical basis for  $^{164}$ Er; the log scale is used for the abscissa. The panel (a) is for neutron and (b) for proton. The spherical oscillator shells  $N_{\rm osc}^{\rm max} = 18$  is used.

First of all, we show the occupation probability of the canonical basis in Fig. 1 in the logarithmic scale, which is a measure how important each canonical orbit is. Not only the occupation probability  $v_k^2$  but the empty probability  $u_k^2 = 1 - v_k^2$  are shown. The quantity  $v_k^2$  quickly decreases after k > N = 96 for neutron and k > Z = 68 for proton. The truncation of the model space is based on the smallness of the occupation probability as is explained in § II C. On the other hand, the quantity  $u_k^2$  tells how important the pairing correlation is for deep hole states. As explained in § II E a part of calculations can be simplified for the orbits with small  $u_k^2$ . As explained in details in § II, the projection calculation is composed of many matrix manipulations. The dimension of the matrices are determined by the model space truncation and, partly, by excluding the core contributions.

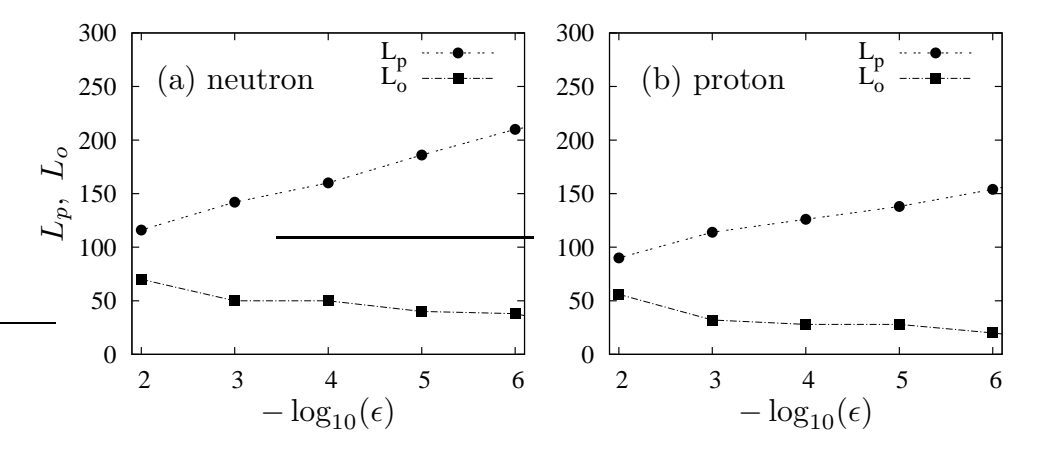


FIG. 2: The number of levels in the model space (P-space)  $L_p$  and the number of core levels  $L_o$  as functions of the small number  $\epsilon$  for  $^{164}$ Er; the log scale is used for the ordinate. The panel (a) is for neutron and (b) for proton. The spherical oscillator shells  $N_{\text{osc}}^{\text{max}} = 18$  is used.

The sizes of the model space  $L_p(\epsilon)$ , the number of orbits k which satisfies  $v_k^2 < \epsilon$  defined in § II C, and the size of the core space  $L_o(\epsilon)$ , the number of orbits k which satisfies  $u_k^2 < \epsilon$  defined in § II E are presented in Fig. 2. As it is clear from the figure, the number  $L_p(\epsilon) - L_o(\epsilon)$  is very small compared to, e.g., the number M = 2660 corresponding to the full size of the oscillator space with  $N_{\text{osc}}^{\text{max}} = 18$ .

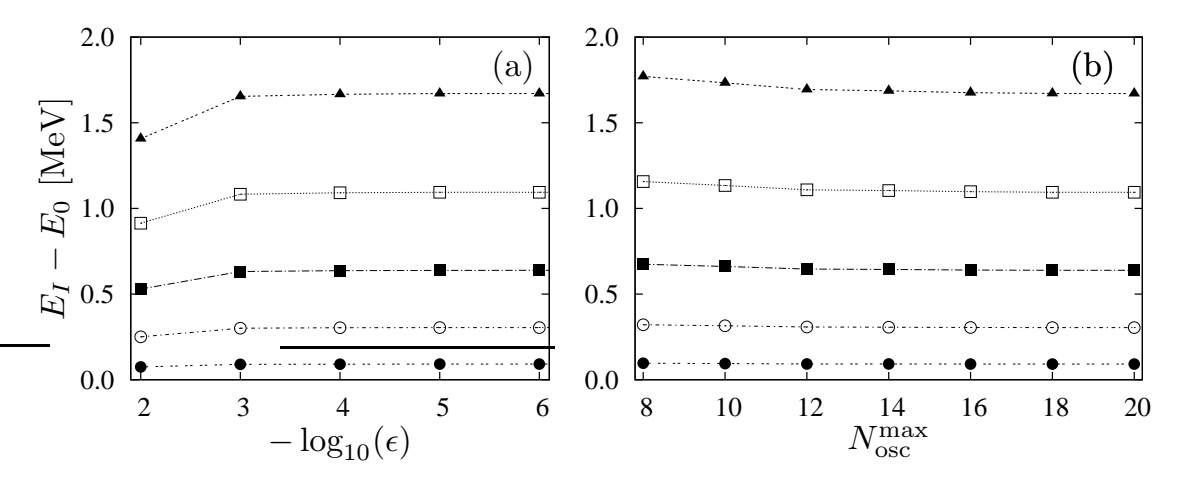


FIG. 3: The rotational excitation spectra from I=2 to 8 calculated by the angular momentum projection for  $^{164}{\rm Er}$  as functions of the cut-off parameter  $\epsilon$  (panel (a)) with  $N_{\rm osc}^{\rm max}=18$ , and of the size of the spherical harmonic oscillator basis  $N_{\rm osc}^{\rm max}$  (panel (b)) with  $\epsilon=10^{-6}$ . The cranking frequency  $\hbar\omega_{\rm rot}=0.01$  MeV is used.

In order to see how the truncated model space can be chosen, we show in the left panel of Fig. 3 the final rotational spectra as functions of the cut-off parameter  $\epsilon$ . It is clear that  $\epsilon \approx 10^{-4}-10^{-5}$  is enough to obtain the convergent results. If we take  $\epsilon \approx 10^{-4}$ ,  $L_p \approx 160~(130)$  and  $L_o \approx 50~(30)$  for neutron (proton). Therefore the size of reduction of model space from  $M=2660~(N_{\rm osc}^{\rm max}=18)$  to  $L_p-L_o$  is about factor 25 in this case. In the right panel of Fig. 3 the convergence of the same rotational spectra with respect to the size of the spherical harmonic oscillator space,  $N_{\rm osc}^{\rm max}$ , is shown. The basis truncation of  $N_{\rm osc}^{\rm max}=10-12$  has been done sometimes for the mean-field calculations. However, the convergence is not enough for higher spin states, and the larger size  $N_{\rm osc}^{\rm max}\approx 18$  is necessary for obtaining the stable excitation energy for the I=8 member. In the following the results with  $\epsilon=10^{-6}$ ,  $N_{\rm osc}^{\rm max}=18$  and  $\hbar\omega_{\rm rot}=0.01$  MeV are shown if the values of them are not explicitly mentioned.

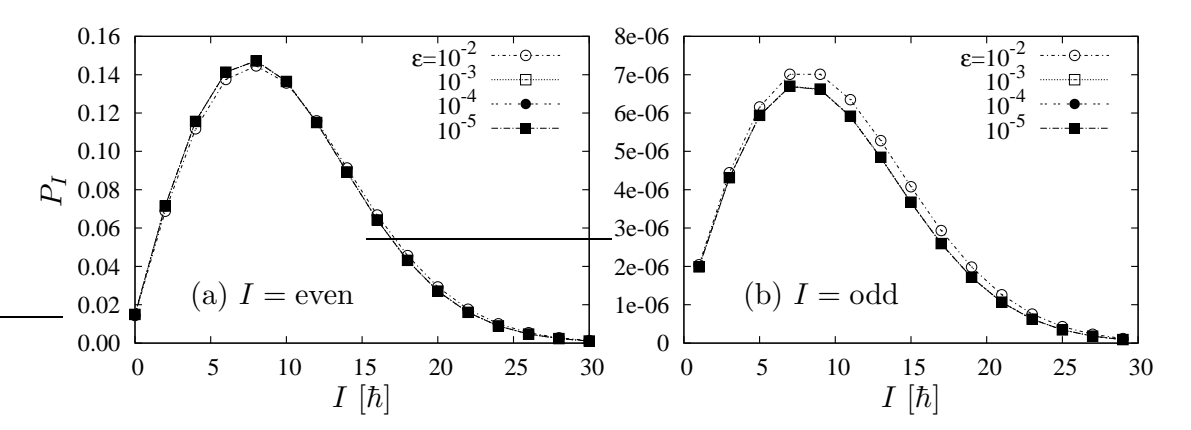


FIG. 4: The I distribution of the mean-field state for  $^{164}$ Er. The cranking frequency is  $\hbar\omega_{\rm rot}=0.01$  MeV. Even and odd I distributions are plotted separately, because the absolute values are very different. Four cases with different values of the cut-off parameter  $\epsilon$  are included.

Although it is already rather well-known, we show in Fig. 4 the distribution of the angular momentum I in the mean-field state  $|\Phi\rangle$ , namely,

$$P_{I} \equiv \sum_{K} \langle \Phi | \hat{P}_{KK}^{I} | \Phi \rangle / \langle \Phi | \Phi \rangle. \tag{121}$$

The results with several  $\epsilon$  values are also included: Again  $\epsilon = 10^{-4}$  is enough for converged results. It is noticed that the probability of having the odd I components is non-zero because the mean-field state is cranked with small frequency  $\omega_{\rm rot} = 0.01$  MeV. If is used

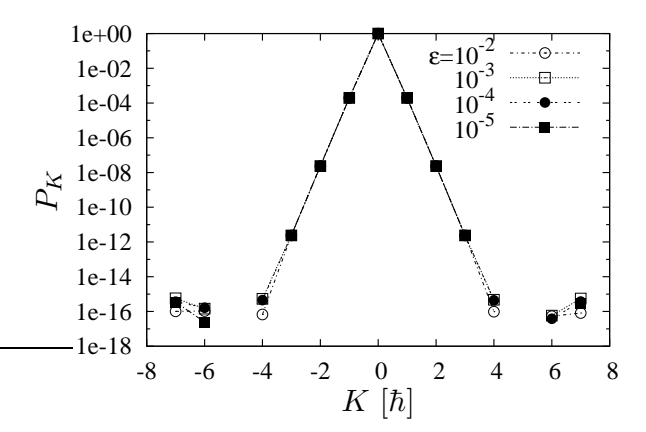


FIG. 5: The K distribution of the mean-field state for  $^{164}$ Er; the log scale is used for the abscissa. The cranking frequency is  $\hbar\omega_{\rm rot}=0.01$  MeV. Four cases with different values of the cut-off parameter  $\epsilon$  are included.

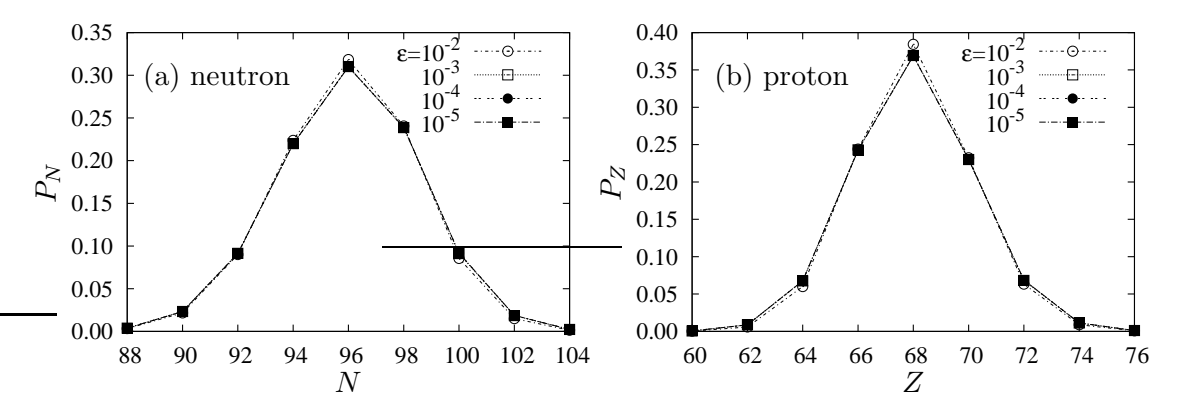


FIG. 6: The number distributions of the mean-field state for  $^{164}$ Er, the panel (a) is for neutron and (b) for proton. Four cases with different values of the cut-off parameter  $\epsilon$  are included.

the non-cranked state, the odd I components are strictly zero because of the signature symmetry (invariance of the  $\pi$  rotation about the cranking axis) and time reversal symmetry present in the axially symmetric mean-field state. Next, the distribution of the K quantum number is shown in Fig. 5:

$$P_K \equiv \sum_{I} \langle \Phi | \hat{P}_{KK}^I | \Phi \rangle / \langle \Phi | \Phi \rangle. \tag{122}$$

The K mixing in the wave function is also due to the Coriolis coupling caused by the cranking procedure; namely the distribution has only K=0 component if the non-cranked mean-field state is used. Since the cranking frequency is small  $\hbar\omega_{\rm rot}=0.01$  MeV,

the distribution of K is almost linear in |K| in the logarithmic scale. Although the mixing of K is very small, it is shown that this  $\Delta K = \pm 1$  mixing is very important to obtain the proper value of the moment of inertia. For completeness, we also show the particle number distributions related to the number projection in Fig. 6;

$$P_N \equiv \langle \Phi | \hat{P}^N | \Phi \rangle / \langle \Phi | \Phi \rangle, \qquad P_Z \equiv \langle \Phi | \hat{P}^Z | \Phi \rangle / \langle \Phi | \Phi \rangle. \tag{123}$$

The main component corresponding to the correct neutron or proton number has about 30-40% probability, which is known to be rather standard for the pairing model space employed presently and for the typical pairing gap  $\Delta \approx 1$  MeV.

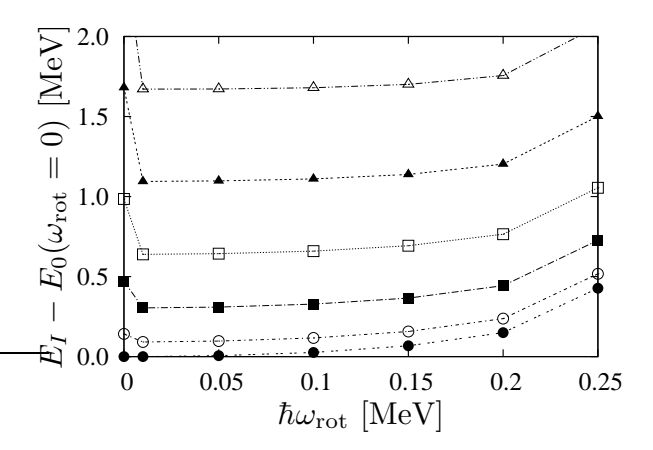


FIG. 7: The rotational excitation spectra obtained by the angular momentum projection from the cranked mean-field state  $|\Phi(\omega_{\rm rot})\rangle$  in  $^{164}{\rm Er}$ .

Now we discuss the effect of the cranking on the spectra obtained by the angular momentum projection. The cranking procedure is an efficient method to study the high spin properties of atomic nuclei. However, we concentrate in this paper on the most fundamental rotational spectra, i.e., those of the ground state band. Therefore we only consider the small cranking frequency so that the two quasiparticle alignment does not occur. We present the resultant spectra obtained by the angular momentum projection from the cranked mean-field state with the frequency  $\omega_{\rm rot}$  in Fig. 7. It is clear that the effect of cranking is very regular and all the energy  $E_I(\omega_{\rm rot})$  with I=0,2,...,10 increases gradually. However, the excitation spectra  $E_I(\omega_{\rm rot}) - E_0(\omega_{\rm rot})$  is essentially identical at least in the range  $0 < \hbar \omega_{\rm rot} < 0.2$  MeV. This indicates that all the cranked mean-field states with  $0 < \hbar \omega_{\rm rot} < 0.2$  MeV are roughly equivalent to generate the ground

state rotational band. We would like to stress that the state with  $\omega_{\rm rot}=0$  does not share this feature; apparently there are discontinuities in the spectra in Fig. 7, namely  $\lim E_I(\omega_{\rm rot}\to 0) \neq E_I(\omega_{\rm rot}=0)$ . Note that the moment of inertia of the first  $2^+$  state,  $3/(E_2(\omega_{\rm rot})-E_0(\omega_{\rm rot}))$ , takes a value  $32.9~\hbar^2/{\rm MeV}$ , while the corresponding value for the non-cranked axially symmetric (only K=0) mean-field is  $21.3~\hbar^2/{\rm MeV}$ , which is much smaller. Therefore the  $\Delta K=\pm 1$  Coriolis coupling effect in the wave function is very important to increase the moment of inertia. It has been known that the cranked mean-field is obtained approximately by the variation after angular momentum projection [1]. Therefore, the cranking procedure is a simple and efficient way to recover the correct moment of inertia even with the angular momentum projection.

The discontinuity of the spectra obtained by projection from the cranked and noncranked spectra can be traced back to the general eigenvalue problem in Eq. (116); discarding the other projectors and the configuration mixing, it reads, for eigenvalue  $E_I$ ,

$$\det\left(\mathcal{H}_{KK'}^{I} - E_{I}\mathcal{N}_{KK'}^{I}\right) = 0, \tag{124}$$

with

$$\begin{pmatrix} \mathcal{H}_{KK'}^I \\ \mathcal{N}_{KK'}^I \end{pmatrix} = \langle \Phi | \begin{pmatrix} \hat{H} \\ 1 \end{pmatrix} \hat{P}_{KK'}^I | \Phi \rangle. \tag{125}$$

In the case of the axially symmetric even-even nuclei, the signature is a good quantum number, and the following reduced kernels can be used with restriction  $K, K' \geq 0$ ,

$$\begin{pmatrix}
\widetilde{\mathcal{H}}_{KK'}^{I} \\
\widetilde{\mathcal{N}}_{KK'}^{I}
\end{pmatrix} \equiv \frac{1}{2\sqrt{(1+\delta_{K0})(1+\delta_{K'0})}} \times \begin{pmatrix}
\mathcal{H}_{KK'}^{I} + (-1)^{I}\mathcal{H}_{K,-K'}^{I} + (-1)^{I}\mathcal{H}_{-K,K'}^{I} + \mathcal{H}_{-K,-K'}^{I} \\
\mathcal{N}_{KK'}^{I} + (-1)^{I}\mathcal{N}_{K,-K'}^{I} + (-1)^{I}\mathcal{N}_{-K,K'}^{I} + \mathcal{N}_{-K,-K'}^{I}
\end{pmatrix}, (126)$$

namely, the dimension of the generalized eigenvalue problem is then (I+1) in place of (2I+1). Now let us consider the problem in the perturbation theory with respect to the rotational frequency  $\omega_{\rm rot}$ . Taking into account the fact that the mean-field state at  $\omega_{\rm rot} = 0$  has only K=0 component, the cranked state is expanded as in the following,

$$|\Phi(\omega_{\text{rot}})\rangle = |\Phi_0(K=0)\rangle + \omega_{\text{rot}}(|\Phi_1(K=+1)\rangle + |\Phi_1(K=-1)\rangle) + \omega_{\text{rot}}^2(|\Phi_2(K=+2)\rangle + |\Phi_2(K=0)\rangle + |\Phi_2(K=-2)\rangle) + ...,$$
 (127)

where  $|\Phi_0(K=0)\rangle \equiv |\Phi(\omega_{\rm rot}=0)\rangle$ , and so are the reduced kernels,

$$\widetilde{\mathcal{H}}_{KK'}^{I} - E_{I} \widetilde{\mathcal{N}}_{KK'}^{I} = \sum_{n=0,2,4,\dots} \omega_{\text{rot}}^{K+K'+n} \left( h_{KK'}^{I(n)} - E_{I} n_{KK'}^{I(n)} \right), \quad (K, K' \ge 0),$$
(128)

with O(1) quantities  $h_{KK'}^{I(n)}$  and  $n_{KK'}^{I(n)}$ . Because of this  $\omega_{\text{rot}}$  dependence, it can be easily confirmed that the determinant can be written as

$$\det\left(\widetilde{\mathcal{H}}_{KK'}^{I} - E_{I}\widetilde{\mathcal{N}}_{KK'}^{I}\right) = \omega_{\text{rot}}^{2(I+1)} \det\left(h_{KK'}^{I(0)} - E_{I}n_{KK'}^{I(0)}\right) + O(\omega_{\text{rot}}^{2(I+2)}), \tag{129}$$

and the eigenvalue equation in Eq. (124) reduces, in the limit  $\omega_{\rm rot} \to 0$ , to

$$\det\left(h_{KK'}^{I(0)} - E_I n_{KK'}^{I(0)}\right) = 0. \tag{130}$$

In contrast, if we put  $\omega_{\text{rot}} = 0$  beforehand in Eq. (128), only K = K' = 0 kernels survives, and we obtain simply the equation,

$$h_{00}^{I(0)} - E_I n_{00}^{I(0)} = \mathcal{H}_{00}^I - E_I \mathcal{N}_{00}^I = 0, \tag{131}$$

which gives the trivial solution  $E_I = \mathcal{H}_{00}^I/\mathcal{N}_{00}^I$ . In this way, the structure of the eigenvalue problem is completely different for  $\omega_{\rm rot} \neq 0$ , and this is the source of the discontinuity of the rotational spectra seen in Fig. 7 in the  $\omega_{\rm rot} \to 0$  limit.

Finally in Fig. 8, we compare the experimental rotational spectra with the results of the quantum number projection calculation. Here we also included the result of an approximation without cranking, and that with neglecting the quadrupole pairing ( $\lambda = 2$ ) component in the  $H_G$  interaction. As it is already pointed out the cranking procedure is important to obtain the correct moment of inertia. The effect of the quadrupole pairing interaction is also considerable, and the moment of inertia can be reproduced only within 20% without it. It should be mentioned that the calculated moment of inertia for high spin members are underestimated. In experiment it is known that the moment of inertia increases as a function of spin; the amount of increase is about 20% at I = 10 in  $^{164}$ Er. However, the calculated moment of inertia is fairly constant for high spin members. The effect of rotation on the mean-field should be included to obtain the proper amount of increase of the moment of inertia, which is a future problem.

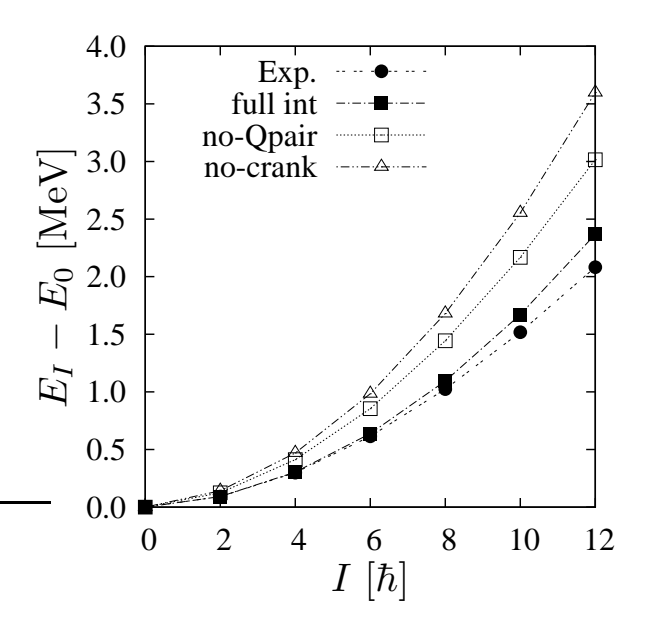


FIG. 8: Comparison of the experimental rotational spectra with the calculated results with various approximations in <sup>164</sup>Er.

## D. Parity doublet bands in <sup>226</sup>Th

The next example is also a typical rotational spectrum but with parity violation. There are several places in nuclear chart, where the static octupole deformation ( $\alpha_{30}$ ) is expected [38]. We take a nucleus <sup>226</sup>Th from the actinide region, which exhibits a nice rotational spectra with alternating parity based on the parity doublet bands. The parameters are chosen in the same ways as in the previous example in <sup>164</sup>Er; especially we took the same value for the ratio of quadrupole and mono pole pairing force strengths. The additional deformation parameter is  $\alpha_{30}$ , which is chosen to reproduce the splitting of the parity doublet bands near the band heads. The resultant parameters are summarized in Table II. The value of  $\alpha_{30}$  is found to be consistent with the calculation in Ref. [38]. The numbers of points for the Gaussian quadrature with respect to the Euler angles are  $N_{\alpha} = N_{\gamma} = 12$ ,  $N_{\beta} = 60$ , and to the gauge angle  $N_{\varphi} = 21$ . As is discussed in the previous section the Coriolis coupling is necessary to reproduce the moment of inertia even for the low lying spectra, so that we use the small cranking frequency  $\omega_{\text{rot}} = 0.01$  MeV in all the calculations.

In Figures 9 and 10, we show the occupation probabilities of the canonical basis and the

$\alpha_{20}$	$\alpha_{30}$	$\alpha_{40}$	$\chi  [\mathrm{MeV^{-1}}]$	$\Delta_{\rm n} \ [{ m MeV}]$	$\Delta_{\rm p} \; [{ m MeV}]$	$g_0^{\rm n} \; [{ m MeV}]$	$g_0^{\rm p} \; [{ m MeV}]$	$g_2^{ au}/g_0^{ au}$
0.164	0.075	0.092	$1.732 \times 10^{-4}$	0.814	0.830	0.1140	0.1583	13.60

TABLE II: The parameters used in the calculation for  $^{226}_{90}\mathrm{Th}_{136}$ . The values of  $\chi$  and  $g_0^{\tau}$  are those for the size of basis  $N_{\mathrm{osc}}^{\mathrm{max}}=18$ .

dimensions of the truncated model (core) space  $L_p$  ( $L_o$ ) for <sup>226</sup>Th, respectively, as in the previous example. It is apparent that the pairing correlations are not so strong that the number of canonical orbits strongly contributing is a few hundreds and rather small. The neutron number N=136 is relatively large, and so is the size of the core space,  $L_o\approx 80$  for  $\epsilon\approx 10^{-4}$ . Although the quantity  $L_p$  is also rather large compared to the previous case of <sup>164</sup>Er, the difference  $L_p-L_o$  is not very different from that of <sup>164</sup>Er. Therefore, the method to separate the core contribution in §IIE helps to reduce the numerical tasks considerably. In this way it has been shown that the method of general quantum number projections developed in §II is very efficient especially when applied to heavier nuclei.

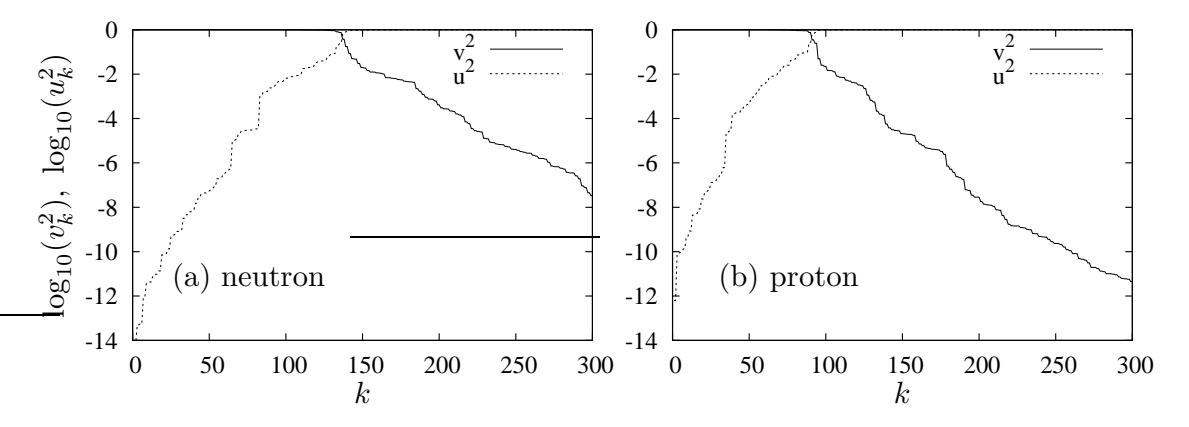


FIG. 9: Occupation and empty probabilities  $v_k^2$  and  $u_k^2 = 1 - v_k^2$  as functions of the number k of the canonical basis for  $^{226}$ Th; the log scale is used for the abscissa. The panel (a) is for neutron and (b) for proton.

In the case of the static octupole deformation the mean-field states mix the parity, and the parity projection is necessary. Because of the signature and time reversal symmetry in the axially symmetric ground state the even (odd) spin is only allowed for positive (negative) parity states. The convergence of the final rotational spectra for each parity against the cut-off parameter  $\epsilon$  is shown in Fig. 11. As in the case of <sup>164</sup>Er the value

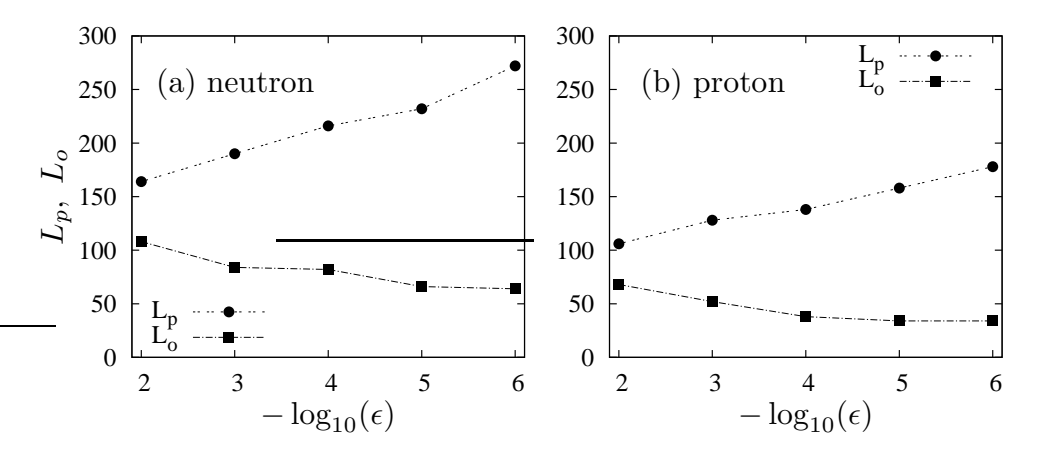


FIG. 10: The number of levels in the model space (P-space)  $L_p$  and the number of core levels  $L_o$  as functions of the small number  $\epsilon$  for  $^{226}$ Th; the log scale is used for the ordinate. The panel (a) is for neutron and (b) for proton.

of  $\epsilon \approx 10^{-4}$  is almost enough to attain the stable results for both  $\pi = \pm$ . In Fig. 12 the projected spectra are shown as functions of the size of the spherical oscillator basis  $N_{\rm osc}^{\rm max}$ . It can be seen that the convergence with respect to  $N_{\rm osc}^{\rm max}$  is slower for the negative parity states, which have generally higher excitation energies.  $N_{\rm osc}^{\rm max} = 18$  is almost enough for the positive parity states, while it may not for the negative parity high spin states. The small oscillator space like  $N_{\rm osc}^{\rm max} = 10$  is dangerous because the energy of 1<sup>-</sup> state is overestimated by more than 200 keV, although the first 2<sup>+</sup> is almost correct; the confirmation of the convergence with respect to the basis size is important.

In Fig. 13 is shown the *I* distributions of the parity broken mean-field state in  $^{226}$ Th. Only the converged results are included for both parities  $\pi = \pm$ :

$$P_{I^{\pm}} \equiv \sum_{K} \langle \Phi | \hat{P}_{KK}^{I} \hat{P}_{\pm} | \Phi \rangle / \langle \Phi | \Phi \rangle. \tag{132}$$

The pattern of the distribution is similar to the case of  $^{164}\text{Er}$ , however, the values of the normal parity components, I=even for  $\pi = +$  or I=odd for  $\pi = -$ , in  $^{226}\text{Th}$  are about half of those in  $^{164}\text{Er}$ . This is because that the mean-field  $|\Phi\rangle$  contains both  $\pi = \pm$  states with almost equal probabilities. Again the non-normal parity components are much smaller than the normal parity components because of the cranking procedure with small frequency  $\omega_{\text{rot}} = 0.01 \text{ MeV}$ .

The quantum number projection from the symmetry broken mean-field states are

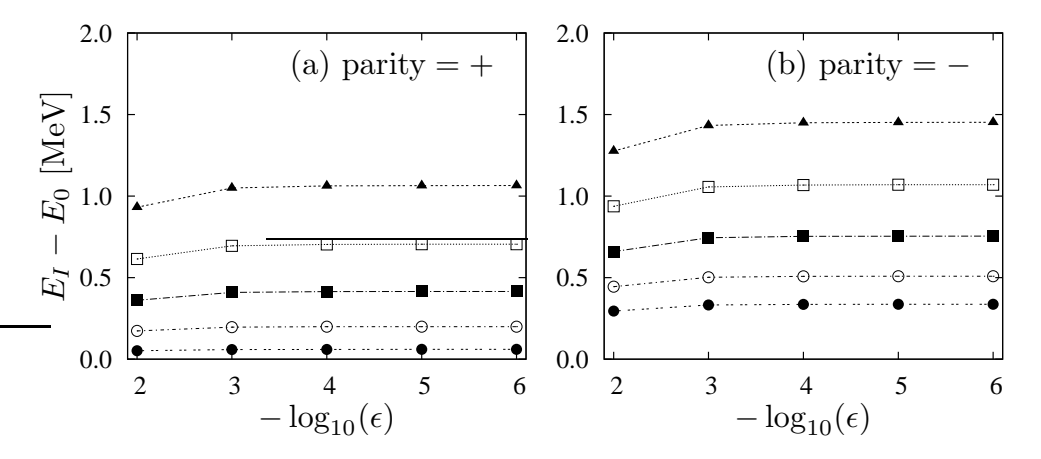


FIG. 11: The rotational excitation spectra calculated by the angular momentum projection for  $^{226}$ Th as functions of the cut-off parameter  $\epsilon$ . The states from I=2 to 8 for  $\pi=+$  and those from I=1 to 7 for  $\pi=-$  are included. The mean-field state with  $N_{\rm osc}^{\rm max}=18$  and  $\hbar\omega_{\rm rot}=0.01$  MeV is used.

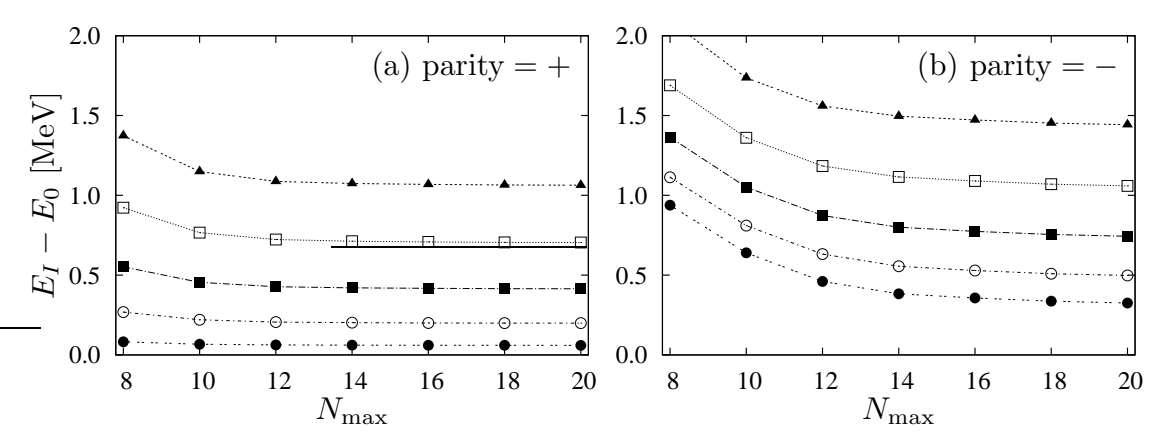


FIG. 12: The rotational excitation spectra calculated by the angular momentum projection for  $^{226}$ Th as functions of the size of the spherical harmonic oscillator basis  $N_{\rm osc}^{\rm max}$ . The states from I=2 to 8 for  $\pi=+$  and those from I=1 to 7 for  $\pi=-$  are included. The cranking frequency  $\hbar\omega_{\rm rot}=0.01$  MeV is used.

known to be an efficient method to include the correlations with respect to the collective motions related to the symmetry, e.g., the rotational correlations in the case of the angular momentum projection. In order to show how much correlation energies can be gained in this particular case, we depict the correlation energies in Fig. 14. The energy gain by the parity projection is not large and less than a few hundred keV, while those

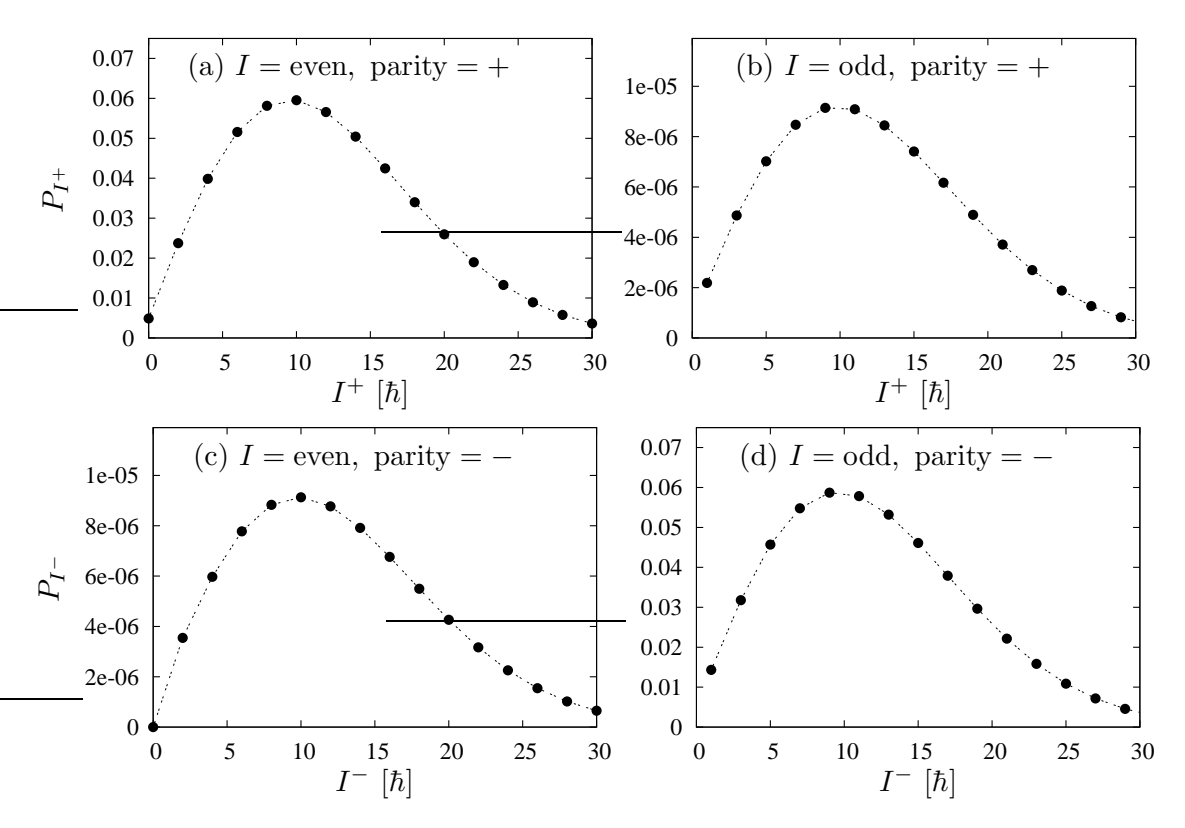


FIG. 13: The I distribution of the mean-field state in  $^{226}$ Th. The cranking frequency is  $\hbar\omega_{\rm rot}=0.01$  MeV. Even and odd I distributions for  $\pi=\pm$  are plotted separately, because the absolute values are very different.

by the number projection (adding the contributions from both neutron and proton) and the angular momentum projection are about 1.5 MeV and 3.0 MeV, respectively, and the total amount is -4.35 MeV in this calculation.

Finally we compare the  $\pi=\pm$  rotational spectra with experimental data in Fig. 15. In this calculation one cranked mean-field with  $\omega_{\rm rot}=0.01$  MeV is used to generate all the states shown in the figure. As is similar to the case of  $^{164}{\rm Er}$ , the experimental moment of inertia increases as a function of spin. The calculated inertia also increases slightly but far not enough to account for the experimentally observed trend. Especially, the degeneracy of the negative and positive parity band becomes better and better for  $I \geq 10$ , which is not well reproduced in the calculation, where the moment of inertia of the high spin part of the negative parity band is too small. The present investigation is the simplest in the sense that only the one intrinsic state is used for all the spins. We need to improve the

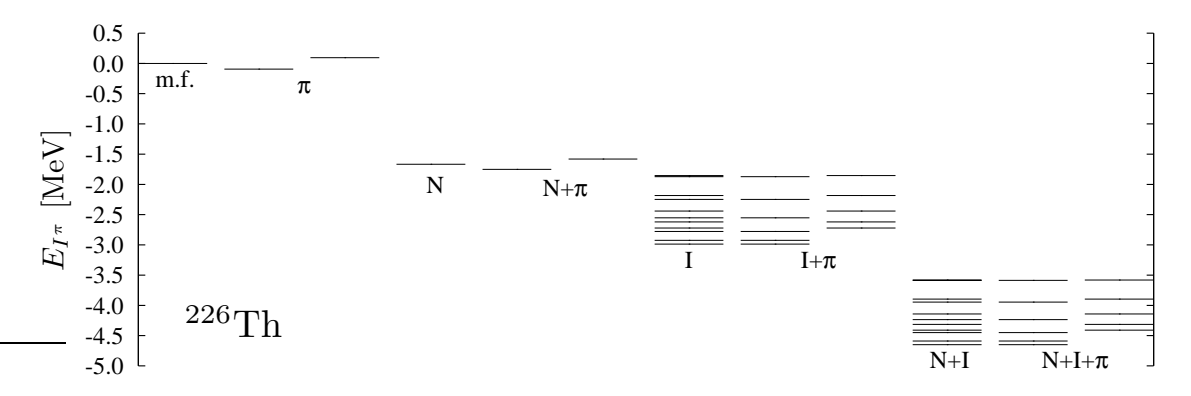


FIG. 14: The energy gain by each projection procedure in  $^{226}$ Th; the parity  $(\pi)$ , the number (N), and the angular momentum (I) projections are done separately as is shown in the figure. For the results of parity projection, the left side spectra are of  $\pi = +$  and the right side  $\pi = -$ . The origin of the energy is that of the mean-field state indicated by "m.f.".

description for the high spin states.

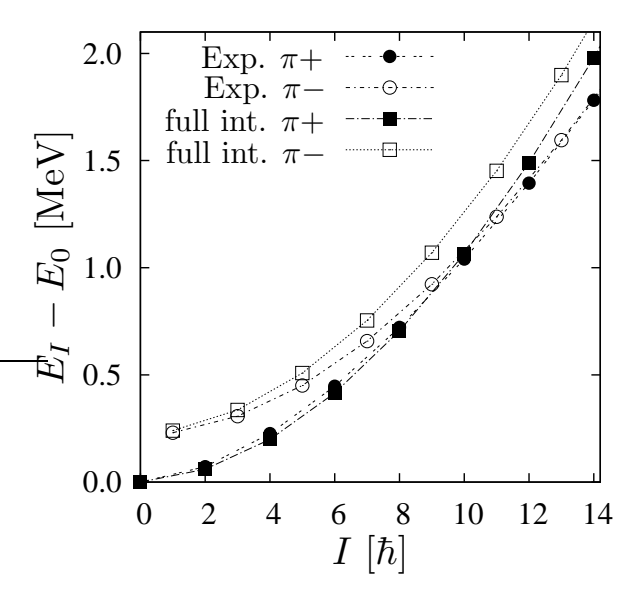


FIG. 15: Comparison of the experimental rotational spectra with the calculated results in  $^{226}$ Th.

## IV. SUMMARY

In this paper, we have developed an efficient technique to perform calculations of the quantum number projections from the most general HFB type state; the the configuration mixing can be done additionally with the same technique if necessary. The use of the HFB type mean-field, i.e., including the effect of the pairing correlation, generally requires a large model space in realistic situations. Our basic strategy is to transform the original basis into the canonical basis, and to discard the orbits with small occupation probabilities. We have shown that the truncation scheme works very well, i.e., the convergence is very rapid and the number orbits which should be included in the calculation is reduced more than an order of magnitude. With this truncation scheme, it has been demonstrated that the angular momentum projection calculation with the spherical oscillator shell more than  $N_{\text{osc}}^{\text{max}} = 20$  is possible.

Another characteristic feature of our approach is that the Thouless amplitude with respect to a Slater determinant is utilized for the projection and configuration mixing calculations. In this way the calculations are divided into the part related to the Slater determinant and the part taking into account the pairing correlation. With this technique, the Thouless amplitude never diverges for the case of small pairing correlations, or for the case where the blocked levels exist, e.g., for the odd nuclei, and calculation can be performed reliably. Moreover, this makes it possible to exclude the core contributions for the pairing correlation and to further reduce the dimension of the various matrix operations. It has been demonstrated that this elimination of the core contribution is especially effective for heavy nuclei like in the actinide region.

As for the test calculations, we have set up the schematic separable interactions suitable for the Woods-Saxon potential, and performed realistic calculations for a rare earth and an actinide nucleus. The quadrupole pairing interaction is included for the pairing channel. The number as well as the angular momentum projections have been done at the same time. In this paper we have used only one mean-field state (no configuration mixing), and tried to describe the typical rotational spectra with good agreements for the low spin states. It has been shown that the cranking with small frequency in the mean-field is very important to reproduce the experimental value of moment of inertia. In the case of the actinide nucleus <sup>226</sup>Th, which is believed to have a pear shape, the parity projection has been also done simultaneously. With a reasonable octupole deformation parameter, the excitation energy of the negative parity band head can be reproduced. However, the calculated moment of inertia with one intrinsic state is almost constants

within the rotational band and does not well describe its gradual increase at higher spin states observed in experiments. Therefore, the effect of change of the mean-field or of the configuration mixing is necessary to obtain a better description of higher spin states, which is an important future problem.

## V. ACKNOWLEDGEMENTS

This work is supported by Grant-in-Aid for Scientific Research (C) No. 22540285 from Japan Society for the Promotion of Science.

## VI. APPENDIX

In this Appendix, we show that the model space truncation scheme, which was first introduced in the Appendix of Ref. [25] in terms of the (U, V) amplitudes, can be naturally derived from our formulation in §II. Note that this can be done without any problem when the truncated dimensions of the left and right states are the same, i.e.,  $L_p = L_{p'}$  (see also [17] and the Appendix of Ref. [20]). We assume it throughout in this Appendix.

The basic quantities that should be evaluated in the projection are the overlap of the transformation operator  $\langle \Phi | \hat{D} | \Phi' \rangle$ , and the associated contractions of the creation and annihilation operators in Eq. (31), which are calculated through those with respect to the canonical basis in Eq. (44). Here we assume that the HFB type states  $|\Phi\rangle$  and  $|\Phi'\rangle$  are normalized. Then by using the normalization constants in Eq. (6) and the  $(\bar{U}, \bar{V})$  amplitudes in the canonical basis in Eq. (17), the overlap in Eq. (42) can be calculated as

$$\langle \Phi | \hat{D} | \Phi' \rangle = e^{i(\theta'_1 - \theta_1)} \langle |\hat{D}| \rangle \left( \det \left( \bar{U}_{pp}^{\dagger} \bar{U}_{p'p'}^{\prime} \right)^* \det \left[ 1 + Z_{pp}^{\dagger} Z_{Dpp}^{\prime} \right] \right)^{1/2}$$

$$= e^{i(\theta'_1 - \theta_1)} \langle |\hat{D}| \rangle \left( \det \left( \bar{U}_{pp}^{\dagger} \bar{U}_{p'p'}^{\prime} \right)^* \det \left[ \tilde{D}_{pp'}^{-T} + Z_{pp}^{\dagger} \tilde{D}_{pp'} Z_{p'p'}^{\prime} \right] \det \left( \tilde{D}_{pp'}^{T} \right) \right)^{1/2}$$

$$= e^{i(\theta'_1 - \theta_1)} \langle |\hat{D}| \rangle \left( \det \tilde{D}_{pp'} \det A_{pp'} \right)^{1/2}, \qquad (133)$$

where  $\theta'_1$  and  $\theta_1$  are the arbitrarily chosen phases for the states  $|\Phi\rangle$  and  $|\Phi'\rangle$ , respectively. In Eq. (133) are used the definitions of the Z amplitude in Eq. (26) and of the  $Z'_D$  in Eq. (41), and the new matrix  $A_{pp'}$  is introduced by

$$A_{pp'} \equiv \bar{U}_{pp}^T \tilde{D}_{pp'}^{-T} \bar{U}_{p'p'}^{\prime*} + \bar{V}_{pp}^T \tilde{D}_{pp'} \bar{V}_{p'p'}^{\prime*}. \tag{134}$$

Note that because of  $L_p = L_{p'}$  the inverse of the matrix  $\tilde{D}_{pp'}$  is well defined. In this way, the overlap can be calculated within the P space. However, the sign problem of the square root remains in this form (133).

The contractions in Eq. (44) can be calculated in terms of the  $(\bar{U}, \bar{V})$  amplitudes in the same way:

$$\rho_{Dpp}^{(b)} = Z'_{Dpp} \left[ 1 + Z^{\dagger}_{pp} Z'_{Dpp} \right]^{-1} Z^{\dagger}_{pp} = \tilde{D}_{pp'} Z'_{p'p'} \left[ \tilde{D}_{pp'}^{-T} + Z^{\dagger}_{pp} \tilde{D}_{pp'} Z'_{p'p'} \right]^{-1} Z^{\dagger}_{pp} 
= \tilde{D}_{pp'} \bar{V}'^{**}_{p'p'} A^{-1}_{pp'} \bar{V}^{T}_{pp},$$
(135)

$$\kappa_{Dpp}^{(b)} = Z'_{Dpp} \left[ 1 + Z^{\dagger}_{pp} Z'_{Dpp} \right]^{-1} = \tilde{D}_{pp'} Z'_{p'p'} \left[ \tilde{D}_{pp'}^{-T} + Z^{\dagger}_{pp} \tilde{D}_{pp'} Z'_{p'p'} \right]^{-1} \\
= \tilde{D}_{pp'} \bar{V}'^{*}_{p'p'} A^{-1}_{pp'} \bar{U}^{T}_{pp}, \tag{136}$$

$$\bar{\kappa}_{Dpp}^{(b)} = \left[1 + Z_{pp}^{\dagger} Z_{Dpp}^{\prime}\right]^{-1} Z_{pp}^{\dagger} = \tilde{D}_{pp^{\prime}}^{-T} \left[\tilde{D}_{pp^{\prime}}^{-T} + Z_{pp}^{\dagger} \tilde{D}_{pp^{\prime}} Z_{p^{\prime}p^{\prime}}^{\prime}\right]^{-1} Z_{pp}^{\dagger}$$

$$= \tilde{D}_{pp^{\prime}}^{-T} \bar{U}_{p^{\prime}p^{\prime}}^{\prime*} A_{pp^{\prime}}^{-1} \bar{V}_{pp}^{T}, \qquad (137)$$

which are calculated within the P space. By using Eq. (51) we finally obtain

$$\rho_D^{(c)} = DW_{p'}'(\bar{V}_{p'p'}^{\prime*} A_{pp'}^{-1} \bar{V}_{pp}^T) W_p^{\dagger}, \tag{138}$$

$$\kappa_D^{(c)} = DW_{p'}'(\bar{V}_{p'p'}^{\prime*} A_{pp'}^{-1} \bar{U}_{pp}^T) \tilde{D}_{pp'}^{-T} W_{p'}^{\prime T} D^T, \tag{139}$$

$$\bar{\kappa}_{D}^{(c)} = W_{p}^{*} \tilde{D}_{pp'}^{-T} (\bar{U}_{p'p'}^{\prime *} A_{pp'}^{-1} \bar{V}_{pp}^{T}) W_{p}^{\dagger}. \tag{140}$$

Thus all the corresponding quantities can be calculated within the truncated canonical basis in terms of the  $(\bar{U}, \bar{V})$  amplitudes in place of the Thouless amplitudes.

In the general case  $L_p \neq L_{p'}$ , the definitions of the inverse matrices  $\tilde{D}_{pp'}^{-1}$  and  $A_{pp'}^{-1}$  are ambiguous, and more careful analysis is necessary. There is no such difficulty in our formulation in terms of the Thouless amplitudes.

<sup>[1]</sup> P. Ring and P. Schuck, The nuclear many-body problem, Springer, New York (1980).

<sup>[2]</sup> J.-P. Blaizot and G. Ripka, Quantum theory of finite systems, MIT press, Cambridge, Massachusetts, and London (1985).

<sup>[3]</sup> M. Bender, P.-H. Heenen, and P.-G. Reinhard, Rev. Mod. Phys. 75, 121 (2003).

<sup>[4]</sup> S. Aberg, H. Flocard, and W. Nazarewicz, Annu. Rev. Nucl. Part. Sci. 40, 439 (1990).

- [5] S. Frauendorf, Rev. Mod. Phys. **73**, 463 (2001).
- [6] W. Satula and R. Wyss, Rep. Prog. Phys. 68, 131 (2005).
- [7] A. Bohr and B. R. Mottelson, Nuclear Structure, Vol. II Benjamin, New York (1975).
- [8] D. R. Bes and J. Kurchan, The treatment of collective coordinates in many-body systems, World Scientific Lecture Notes in Physics, Vol. 34, World Scientific, Singapore, (1990).
- [9] K. Hara and S. Iwasaki, Nucl. Phys. **A332**, 61 (1979).
- [10] K. Hara, S. Iwasaki, and K. Tanabe, Nucl. Phys. **A332**, 69 (1979).
- [11] K. Hara and S. Iwasaki, Nucl. Phys. **A348**, 200 (1980).
- [12] K. Hara, A. Hayashi, and P. Ring, Nucl. Phys. A385, 14 (1982).
- [13] K. Hara and Y. Sun, Int. J. Mod. Phys. E 4, 637 (1995).
- [14] K. Enami, K. Tanabe, and N. Yoshinaga, Phys. Rev. C 59, 135 (1999).
- [15] K. W. Schmid and F. Grümmer, Rep. Rpog. Phys. **50**, 731 (1987).
- [16] K. W. Schmid, Prog. Part. Nucl. Phys. **52**, 565 (2004).
- [17] A. Valor, P.-H. Heenen, and P. Bonche, Nucl. Phys. **A671**, 145 (2000).
- [18] R. Rodriguez-Guzman, J. L. Egido, and L. M. Robledo, Nucl. Phys. A709, 201 (2002).
- [19] M. Bender and P.-H. Heenen, Phys. Rev. C 78, 024309 (2008).
- [20] J. M. Yao, J. Meng, P. Ring, and D. Pena Arteaga, Phys. Rev. C 79, 044312 (2009).
- [21] J. M. Yao, J. Meng, P. Ring, and D. Vretenar, Phys. Rev. C 81, 044311 (2010).
- [22] T. R. Rogríguez and J. L. Egido, Phys. Rev. C 81, 064323 (2010).
- [23] N. Onishi and S. Yoshida, Nucl. Phys. **80**, 268 (1966).
- [24] R. Balian and E. Brezin, Nuovo Cimento **B64**, 37 (1969).
- [25] P. Bonche, H. Flocard, P.-H. Heenen, adn J. Meyer, Nucl. Phys. **A510**, 466 (1990).
- [26] L. M. Robledo, Phys. Rev. C **50**, 2874 (1994).
- [27] L. M. Robledo, Phys. Rev. C **79**, 021302(R) (2009).
- [28] C. González-Ballestero, L. M. Robledo, and G. F. Bertsch, Comput. Phys. Commun. 182, 2213 (2011).
- [29] N. Tajima, Phys. Rev. C **69**, 034305 (2004).
- [30] L. M. Robledo, Int. J. Mod. Phys. E **16**, 337 (2007).
- [31] J. Dobaczewski, M. Stoitsov, W. Nazarewicz, and P. G. Reinhard, Phys. Rev. C 76, 054315 (2007).

- [32] M. Bender, T. Duguet, and D. Lacroix, Phys. Rev. C 79, 044319 (2009).
- [33] N. Tajima, Y. R. Shimizu, and S. Takahara, Phys. Rev. C 82, 034316 (2010).
- [34] S. Cwiok, J. Dudek, W. Nazarewicz, J. Skalski and T. Werner, Comp. Phys. Comm. 46, 379 (1987).
- [35] R. Wyss, private communication (2005).
- [36] T. Shoji and Y. R. Shimizu, Prog. Theor. Phys. 121, 319 (2009).
- [37] K. Minomo, T. Sumi, M. Kimura, K. Ogata, Y. R. Shimizu, and M. Yahiro, Phys. Rev. C 84, 034602 (2011).
- [38] P. A. Butler and W. Nazarewicz, Rev. Mod. Phys. 68, 349 (1996).

